






A Unified Expression for Upper Bounds on the BLER of Spinal Codes over Fading Channels

Aimin Li , Graduate Student Member, IEEE, Xiaomeng Chen , Shaohua Wu , Member, IEEE, Gary C.F. Lee , Member, IEEE, and Sumei Sun , Fellow, IEEE.

Abstract—Performance evaluation of particular channel coding has been a significant topic in coding theory, often involving the use of bounding techniques. This paper focuses on the new family of *capacity-achieving* codes, Spinal codes, to provide a comprehensive analysis framework to tightly upper bound the block error rate (BLER) of Spinal codes in the finite block length (FBL) regime. First, we resort to a variant of the *Gallager random coding bound* to upper bound the BLER of Spinal codes over the fading channel. Then, this paper derives a new bound without resorting to the use of *Gallager random coding bound*, achieving provable tightness over the wide range of signal-to-noise ratios (SNR). The derived BLER upper bounds in this paper are generalized, facilitating the performance evaluations of Spinal codes over different types of fast fading channels. Over the Rayleigh, Nakagami-m, and Rician fading channels, this paper explicitly derived the BLER upper bounds on Spinal codes as case studies. Based on the bounds, we theoretically reveal that the *tail transmission pattern* (TTP) for ML-decoded Spinal codes keeps optimal in terms of reliability performance. Simulations verify the tightness of the bounds and the insights obtained.

Index Terms—Spinal codes, block error rate (BLER), fading channels, ML decoding, upper bounds, finite block length.

I. INTRODUCTION

A. Background

First proposed in 2011 [2], Spinal codes are a new family of *capacity-achieving rateless* codes [3]. The *capacity-achieving* and *rateless* properties enable Spinal codes with superior performance in ensuring reliable and high-efficiency communications over time-varying channels. In [4], it has demonstrated that Spinal codes outperform Raptor codes [5], [6], Strider codes [7] and *rateless* Low-Density Parity-Check (LDPC) codes [8] in terms of *throughput* across a wide range of channel conditions and message sizes.

Owing to the superior *rateless* and *capacity-achieving* properties, Spinal codes have garnered substantial attention in the realm of coding design, leading to a plethora of research endeavors including Spinal coding structure design [9]–[11], high-efficiency decoding mechanisms [12], [13], compressive Spinal codes [14], punctured Spinal codes [15], [16], timeliness-oriented Spinal codes [17], [18], and Polar-Spinal concatenation codes [19]–[22]. These studies offer deeper insights into Spinal codes. Yet, the *theoretical* analysis, especially within the Finite Block Length (FBL) regime, remains nascent, which constrains their further advancement.

B. Related Works and Motivations

In coding theory, obtaining a closed-form expression for the block error rate (BLER) of channel codes in the FBL regime

is significant. Such expressions facilitate accurate performance evaluations and highlight improvements in coding design. However, obtaining exact closed-form expressions is usually challenging, arising from the intricate, typically non-linear operations involved in the channel coding process. As an alternative, bounds are derived for performance evaluations [23]. Today, many tight bounds have been derived, including upper bounds on Polar codes [24], [25], Turbo codes [26], Raptor codes [27], LT codes [28], [29], and the upper and lower bounds on the error probability of Maximum Likelihood (ML)-decoded linear codes [30]. However, Spinal codes, a new candidate of *capacity-achieving* codes, remains relatively unexplored in terms of deriving *tight, explicit* bounds.

Some works have conducted theoretical analysis of Spinal codes over the AWGN channel and the binary symmetric channel (BSC). In [3], Balakrishnan *et.al.* conducted an asymptotic rate analysis of Spinal codes and proved that Spinal codes are *capacity-achieving* over both the AWGN and the BSC channels. In [9], Yu *et.al.* carried out the FBL analysis of Spinal codes and derived the BLER upper bounds over the AWGN and the BSC channels. The core idea in [9] is an introduction of the *Random Coding Union* (RCU) bound [31, *Theorem 33*] (over the BSC) and a relaxed version of the *Gallager random coding bound* [32, *Theorem 5.6.2*] (over the AWGN) to upper bound Spinal codes. In [33], we further tightened the FBL upper bound over the AWGN channel by characterizing the error probability as the volume of a hypersphere divided by the volume of a hypercube, improving the tightness of the bounds in the high-SNR regime. However, almost all previous works are established over the BSC or AWGN channels. The FBL analysis of Spinal codes over fading channels remains a relatively unexplored area.

In [34], we introduced the *Chernoff bound* to derive the upper bound on the BLER of Spinal codes, with a specific focus on the *Rayleigh* fading channel without channel state information. However, due to the probability-convergent nature of the *Chernoff bound*, the derived bound is contingent upon a *confidence probability*. Consequently, the bound lacks rigorous *explicitness* and its *applicability* is restricted to Rayleigh fading. *In summary, the tight, closed-form, and generalized FBL bound on the BLER of Spinal codes over fading channels remains unresolved. This underscores the need for new techniques, tools, and methodologies.*

C. Main Results and Contributions

Motivated by the above, this paper aims to derive new, *tight, closed-form, and generalized* upper bounds on the BLER of Spinal codes over fading channels. Building upon the earlier version in [1], this work achieves distinctive contributions:

An earlier version of this paper was presented in part at the 2023 IEEE International Symposium on Information Theory (IEEE ISIT 2023) [1].

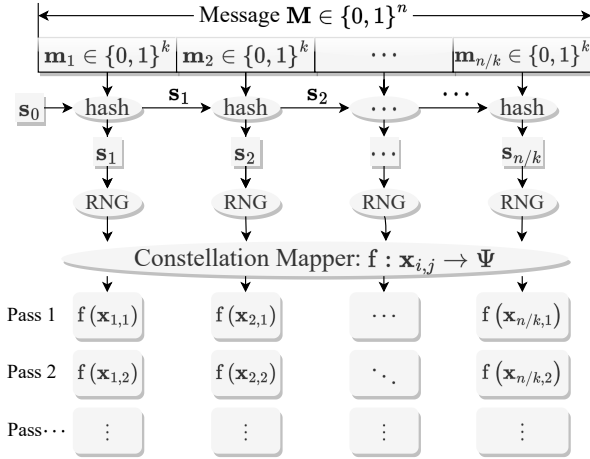


Fig. 1. The encoding process of Spinal codes.

Theory: (1) We derive a new bound in Theorem 1, which is based on the variant of *Gallager random coding bound*. We find that compared to the bound based on the variant of *Gallager random coding bound*, our approach in Theorem 2 provably achieves tighter evaluations. (2) We unified the derived bounds in [1] into a cohesive framework. Upper bounds over different fading channels are unified into a compact, generalized expression. (3) Our framework extends beyond the real-number scope of [1] to complex mapping and fading. This represents the first work that analyzes Spinal codes over complex mapping scenarios. To address this challenge, we develop new methods and tools to facilitate the analysis.

Optimization: Building upon the theoretical analysis, we formulate a problem aimed at minimizing the BLER to optimize the transmission pattern of Spinal codes. Initially, a greedy algorithm is proposed to derive the transmission pattern. Subsequently, we find that the solutions exhibit a regularity – invariably leading to the tail transmission pattern (TTP). Thus, we explore the optimality of the TTP and establish that the TTP is optimal for ML-decoded Spinal codes. To our knowledge, this is the first work that unveils, through theoretical proof, that transmitting tail symbols can enhance the performance of Spinal codes.

D. Notations

Bold symbols denote vectors or matrices. $\{0, 1\}^v$ denotes a v -length binary sequence. $\Re[\cdot]$ and $\Im[\cdot]$ denote the real and imaginary parts of matrices, vectors, or scalars. $\exp\{\cdot\}$ represents the exponential function. $(\cdot)^H$, $(\cdot)^*$, $\|\cdot\|_n$, $|\cdot|$, and $\Pr(\cdot)$ represents the Hermitian transpose, the complex conjugate, the ℓ^n -norm, the modulus, and the probability. $\mathbb{P}_X(x)$ and $f_X(x)$ represent the probability mass function (PMF) and the probability density function (PDF) of the random variable X , respectively. \mathbb{R} , \mathbb{C} , \mathbb{R}^L , and \mathbb{C}^L denote the real space, complex space, L -dimensional real vector space, and L -dimensional complex vector space, respectively. $\mathbb{E}_X[\cdot]$ represents the expectation in terms of the random variable X . \mathbb{N} and \mathbb{N}^+ denote the set of natural numbers and positive integers, respectively. $\mathcal{N}(\mu, \sigma^2)$ and $\mathcal{CN}(\mu, \sigma^2)$ represent the Gaussian distribution and the symmetric complex Gaussian

distribution with mean μ and variance σ^2 , respectively. $\mathbf{0}^v$ denotes the all-zero length- v vector. For a positive integer n , $[n]$ denotes the set of integers from 1 to n : $[n] \triangleq \{1, 2, \dots, n\}$. $\Gamma(x) \triangleq \int_0^\infty e^{-t} t^{x-1} dt$ denotes the gamma function, $Q(x) \triangleq \frac{1}{\sqrt{2\pi}} \int_x^\infty e^{-\frac{x^2}{2}} dx$ denotes the Q function, and $I_0(x)$ represents the zero-order modified Bessel function of the first kind.

II. PRELIMINARIES

A. Encoding Process of Spinal Codes

This subsection introduces the encoding process of Spinal codes, as shown in Fig. 1. There are five key steps:

- 1) *Segmentation*: Divide an n -bit message M into k -bit segments $m_i \in \{0, 1\}^k$, where $i \in [n/k]$.
- 2) *Sequentially Hashing*: The hash function $\mathcal{H}(\cdot)$ sequentially generates v -bit spine values $s_i \in \{0, 1\}^v$, with

$$s_i = \mathcal{H}(s_{i-1}, m_i), i \in [n/k], s_0 = \mathbf{0}^v. \quad (1)$$

- 3) *RNG*: Each spine value s_i seeds an RNG to generate a binary pseudo-random uniform-distributed sequence $\{\mathbf{x}_{i,j}\}_{j \in \mathbb{N}^+}$. In this sequence, each $\mathbf{x}_{i,j}$ belongs to $\{0, 1\}^c$, where c represents the length of $\mathbf{x}_{i,j}$. Here, i is the index of spines and j is the index of passes.

$$\text{RNG} : s_i \rightarrow \{\mathbf{x}_{i,j}\}_{j \in \mathbb{N}^+}, \quad (2)$$

- 4) *Constellation Mapping*: The constellation mapper maps each c -bit symbol $\mathbf{x}_{i,j}$ to a channel input set Ψ :

$$f : \mathbf{x}_{i,j} \rightarrow \Psi, \quad (3)$$

where f is the constellation mapping function and it converts each c -bit symbol $\mathbf{x}_{i,j}$ to the real space \mathbb{R} or complex space \mathbb{C} for transmission.

The properties of the implemented hash functions are in Appendix A, which lay the foundation for the FBL analysis.

B. Channel Model

We consider the flat fast fading channel, and thus the received symbol $y_{i,j}$ is generally expressed by

$$y_{i,j} = h_{i,j} f(\mathbf{x}_{i,j}) + n_{i,j}, \quad (4)$$

where $f(\mathbf{x}_{i,j}) \in \Psi$ is the coded symbols and $h_{i,j}$ is the corresponding fading coefficient. Under the complex-mapping constellation condition, $n_{i,j}$ follows the symmetric complex Gaussian distribution with $n_{i,j} \sim \mathcal{CN}(0, \sigma^2)$ and the distribution of $h_{i,j}$ are contingent on the type of fading channels.

III. BOUND BASED ON GALLAGER'S RESULTS

The standard *Gallager random coding bound* has been introduced [9, Theorem 4] to upper bound the BLER of Spinal codes over the AWGN channel. However, this standard adaptation encounters limitations when applied to fading channels, hindering the FBL analysis of Spinal codes over fading channels. To address this issue, we introduce an extension of the conventional *Gallager bound*, formulating a variant specifically designed for fading channel conditions.

¹The initial spine value s_0 is known to both the encoder and the decoder and is usually set as $s_0 = 0$ without loss of generality.

$$\begin{aligned}
& \iint_{\mathbb{R}} \left[\sum_{x \in \Psi} \frac{\exp\left\{-\frac{(a - \Re[Hx])^2 + (b - \Im[Hx])^2}{2\sigma^2}\right\}}{\sqrt{\pi\sigma^2}} \right]^2 \text{dadb} \stackrel{\text{(a)}}{=} \frac{\sum_{\beta_i, \beta_j \in \Psi} \iint_{\mathbb{R}} \exp\left\{-\frac{(a - \Re[H\beta_i])^2 + (b - \Im[H\beta_j])^2 + (a - \Re[H\beta_i])^2 + (b - \Im[H\beta_j])^2}{2\sigma^2}\right\}}{\pi\sigma^2} \text{dadb}}{\pi\sigma^2} \\
&= \frac{1}{\pi\sigma^2} \sum_{\beta_i, \beta_j \in \Psi} \int_{\mathbb{R}} \exp\left\{-\frac{(a - \Re[H\beta_i])^2 + (a - \Re[H\beta_j])^2}{2\sigma^2}\right\} \text{da} \times \int_{\mathbb{R}} \exp\left\{-\frac{(b - \Im[H\beta_i])^2 + (b - \Im[H\beta_j])^2}{2\sigma^2}\right\} \text{db} \\
&\stackrel{\text{(b)}}{=} \sum_{\beta_i, \beta_j \in \Psi} \exp\left\{-\frac{(\Re[H\beta_i] - \Re[H\beta_j])^2}{4\sigma^2}\right\} \times \exp\left\{-\frac{(\Im[H\beta_i] - \Im[H\beta_j])^2}{4\sigma^2}\right\} \stackrel{\text{(c)}}{=} \sum_{\beta_i, \beta_j \in \Psi} \exp\left\{-\frac{|H(\beta_i - \beta_j)|^2}{4\sigma^2}\right\} \quad (11)
\end{aligned}$$

A. Gallager Bound over the Fading Channel

In this subsection, the explicit *Gallager bound* over the considered fast flat fading channel will be derived.

Lemma 1. *For channel codes with codelength L , code rate R , and channel input set Ψ , the average BLER is upper bounded by*

$$\Pr\{\mathcal{E}\} \leq \exp\{LR\} \cdot \left\{ \mathbb{E}_H \left[\sum_{\beta_i, \beta_j \in \Psi} \exp\left\{-\frac{|H(\beta_i - \beta_j)|^2}{4\sigma^2}\right\} \right] \right\}^L, \quad (5)$$

where \mathcal{E} represent the event of decoding error, H is the random fading coefficient.

Proof. The *Gallager bound* given a specific fading coefficient H is given as in [35, Eq. (14)]:

$$\Pr\{\mathcal{E}|H\} \leq \min_{\rho \in [0,1]} \left\{ \exp\{LR\} \cdot \left\{ \int_{\mathbb{C}} \left[\sum_{x \in \Psi} \mathcal{Q}(x) f_Y(y|x, H)^{1/(1+\rho)} \right]^{1+\rho} \text{dy} \right\}^L \right\}, \quad (6)$$

where \mathcal{E} is the decoding error, $\mathcal{Q}(x)$ is the distribution of x , $f_Y(y|x, H)$ is the distribution of the received symbol y given x and H . The BLER $\Pr\{\mathcal{E}\}$ can be given as $\Pr\{\mathcal{E}\} = \mathbb{E}_H[\Pr\{\mathcal{E}|H\}]$. With (6), $\Pr\{\mathcal{E}\}$ is upper bounded by

$$\mathbb{E}_H \left[\min_{\rho \in [0,1]} \left\{ \exp\{LR\} \cdot \left\{ \int_{\mathbb{C}} \left[\sum_{x \in \Psi} \mathcal{Q}(x) f_Y(y|x, H)^{1/(1+\rho)} \right]^{1+\rho} \text{dy} \right\}^L \right\} \right]. \quad (7)$$

The complexity in solving (7) lies in optimizing over ρ . To simplify the analysis, we follow a similar approach as in [9, Theorem 2]. Specifically, by applying the inequality $\min_{0 \leq \rho \leq 1} f(\rho) \leq f(1)$ to (7) and rearranging the expectation $\mathbb{E}_H [f(H)^L] = (\mathbb{E}_H [f(H)])^L$ (due to the i.i.d of $h_{i,j}$ in our considered model), $\Pr\{\mathcal{E}\}$ is upper bounded by

$$\Pr\{\mathcal{E}\} \leq \exp\{LR\} \cdot \left\{ \mathbb{E}_H \left[\int_{\mathbb{C}} \left[\sum_{x \in \Psi} \mathcal{Q}(x) \sqrt{f_Y(y|x, H)} \right]^2 \text{dy} \right] \right\}^L. \quad (8)$$

To explicitly determine the right-hand side (RHS) of (8), our remaining focus is to calculate the integral $\mathcal{J} = \int_{\mathbb{C}} \left[\sum_{x \in \Psi} \mathcal{Q}(x) \sqrt{f_Y(y|x, H)} \right]^2 \text{dy}$. This task is intuitively challenging. Our next focus is to demonstrate that this integral can be explicitly solved.

Notably, the distribution of x is $\mathcal{Q}(x) = 2^{-c}$, as discussed in the property of RNG. By substituting $\mathcal{Q}(x) = 2^{-c}$ into

the integral and employing the factorization $f_Y(y|x, H) = f_{\Re[Y]}(\Re[y]|x, H) \cdot f_{\Im[Y]}(\Im[y]|x, H)$ (since $\Re[Y]$ and $\Im[Y]$ are independent with each other), we obtain

$$\mathcal{J} = \frac{\iint_{\mathbb{R}} \left[\sum_{x \in \Psi} \sqrt{f_{\Re[Y]}(\Re[y]|x, H) \cdot f_{\Im[Y]}(\Im[y]|x, H)} \right]^2 \text{d}\Re[y] \text{d}\Im[y]}{2^{2c}}. \quad (9)$$

Given that $\Re[y] = \Re[Hx] + \Re[n]$, $\Im[y] = \Im[Hx] + \Im[n]$, and $\Re[n], \Im[n] \sim \mathcal{N}(0, \sigma^2/2)$, the PDFs of $\Re[y]$ and $\Im[y]$ are

$$\begin{aligned}
f_{\Re[Y]}(\Re[y]|x, H) &= \frac{1}{\sqrt{\pi\sigma^2}} \exp\left\{-\frac{(\Re[y] - \Re[Hx])^2}{\sigma^2}\right\}, \\
f_{\Im[Y]}(\Im[y]|x, H) &= \frac{1}{\sqrt{\pi\sigma^2}} \exp\left\{-\frac{(\Im[y] - \Im[Hx])^2}{\sigma^2}\right\}.
\end{aligned} \quad (10)$$

Let $a = \Re[y]$, $b = \Im[y]$ and apply (10) in (9), (9) turns to (11) at the top of this page, where equality (11-a) holds because $(\sum_i f(i))^2 = \sum_{i,j} f(i)f(j)$, (11-b) is proved in Appendix B-B, and (11-c) is obtained by $|x|^2 = \Re[x]^2 + \Im[x]^2$. Substituting (11) into (8) yields the compact form of *Gallager bound* over the complex fading channel. \square

Corollary 1. *If x , H , and y are real numbers, then the *Gallager bound* turns to*

$$\Pr\{\mathcal{E}\} \leq \exp\{LR\} \cdot \left\{ \mathbb{E}_H \left[\sum_{\beta_i, \beta_j \in \Psi} \exp\left\{-\frac{|H(\beta_i - \beta_j)|^2}{8\sigma^2}\right\} \right] \right\}^L. \quad (12)$$

Proof. The proof is accomplished by re-deriving (8), See Appendix B-A. \square

B. Upper Bound on the BLER of Spinal Codes

With (5) in hand, we can derive the upper bound on the BLER of Spinal codes over fading channels.

Theorem 1. *Consider Spinal codes with message length n , segmentation parameter k , modulation parameter c , channel input set Ψ , and sufficiently large hash parameter v^2 , transmitted over a flat fast complex fading channel with AWGN variance σ^2 , the average BLER given perfect CSI under ML decoding for Spinal codes can be upper bounded by*

$$P_e \leq 1 - \prod_{a \in [n/k]} (1 - \epsilon_a), \quad (13)$$

²In the sequel, we use the shorthand $(n, k, c, \Psi, v \gg 0)$ Spinal codes to denote Spinal codes with such parameter setting.

with

$$\epsilon_a = 2^{k(n/k-a+1)} \cdot \left\{ \mathbb{E}_H \left[\sum_{\beta_i, \beta_j \in \Psi} \exp \left\{ -\frac{|H(\beta_i - \beta_j)|^2}{4\sigma^2} \right\} \right] \right\}^{L_a}, \quad (14)$$

where $H \in \mathbb{C}$ characterizes the channel fading coefficient, $L_a = \sum_{i=a}^{n/k} \ell_i$, ℓ_i is the number of transmitted symbols generated from the spine value \mathbf{s}_i .

Proof. The deviation of the proof compared to that of [9, Theorem 4] stems from substituting [9, Eq. (24)] with (5), which leads to (15). We thus omit the detailed proof here. \square

Corollary 2. *Over the real fading channel, (13) holds and (14) refines to*

$$\epsilon_a = 2^{k(n/k-a+1)} \cdot \left\{ \mathbb{E}_H \left[\sum_{\beta_i, \beta_j \in \Psi} \exp \left\{ -\frac{|H(\beta_i - \beta_j)|^2}{8\sigma^2} \right\} \right] \right\}^{L_a}, \quad (15)$$

Proof. The proof is accomplished by similarly leveraging Corollary 1 to re-derive ϵ_a . We thus omit the proof here. \square

Remark 1. *Our result is an extension of [9, Theorem 4]. When $H \equiv 1$, Corollary 2 reduces to the bound over the AWGN channel obtained in [9, Theorem 4].*

IV. REFINING THE BOUND

In this section, we present a new BLER upper bound for Spinal codes that is provably tighter than Theorem 1.

Theorem 2. *Consider $(n, k, c, \Psi, v \gg 0)$ Spinal codes transmitted over a flat fast complex fading channel with AWGN variance σ^2 , the average BLER given perfect CSI under ML decoding for Spinal codes can be upper bounded by*

$$P_e \leq 1 - \prod_{a \in [n/k]} (1 - \epsilon_a), \quad (16)$$

$$\text{where } \epsilon_a = \min \left\{ 1, (2^k - 1) 2^{n-ak} \cdot \mathcal{F}(L_a, \sigma) \right\}, \quad (17)$$

with $\mathcal{F}(L_a, \sigma)$ equals to

$$\sum_{t \in [N]} b_t \left(\sum_{\beta_i, \beta_j \in \Psi} 2^{-2c} \mathbb{E}_H \left[\exp \left\{ \frac{-|H(\beta_i - \beta_j)|^2}{4\sigma^2 \sin^2 \theta_t} \right\} \right] \right)^{L_a}, \quad (18)$$

where θ_t is arbitrarily chosen with $\theta_0 = 0, \theta_N = \frac{\pi}{2}$ and $\theta_0 < \theta_1 < \dots < \theta_N$, and N represents the number of θ values which enables the adjustment of accuracy.

Proof. Suppose a message $\mathbf{M}^* = (\mathbf{m}_1^*, \mathbf{m}_2^*, \dots, \mathbf{m}_{n/k}^*) \in \{0, 1\}^n$ is encoded to $\mathbf{f}(\mathbf{x}_{i,j}(\mathbf{M}^*)) \in \mathbb{C}$ to be transmitted over a flat fast complex fading channel. At the receiver, the ML rule given perfect CSI is

$$\widehat{\mathbf{M}} \in \arg \min_{\mathbf{M} \in \{0, 1\}^n} \mathcal{D}(\mathbf{M}), \quad (19)$$

where $\mathcal{D}(\cdot) \triangleq \sum_{i \in [n/k]} \sum_{j \in [\ell_i]} |y_{i,j} - h_{i,j} \mathbf{f}(\mathbf{x}_{i,j}(\cdot))|^2$ is the decoding cost and $\widehat{\mathbf{M}} = (\widehat{\mathbf{m}}_1, \widehat{\mathbf{m}}_2, \dots, \widehat{\mathbf{m}}_{n/k}) \in \{0, 1\}^n$ is the decoding result. The ML decoder aims at selecting the one

with the lowest decoding cost from the candidate sequence space $\{0, 1\}^n$. If $\widehat{\mathbf{M}} = \mathbf{M}^*$, the decoding result is correct; otherwise, it is a decoding error.

We categorize the candidate sequence space $\{0, 1\}^n$ into two groups: the correct decoding sequence denoted as \mathbf{M}^* , and the incorrect decoding sequences symbolized as $\mathbf{M}' = (\mathbf{m}'_1, \mathbf{m}'_2, \dots, \mathbf{m}'_{n/k}) \in \mathcal{W}$, with $\mathcal{W} \triangleq \{(\mathbf{m}'_1, \mathbf{m}'_2, \dots, \mathbf{m}'_{n/k}) : \exists 1 \leq i \leq n/k, \mathbf{m}'_i \neq \mathbf{m}_i^*\}$. Given \mathbf{M}^* transmitted, the received signal is $y_{i,j} = h_{i,j} \mathbf{f}(\mathbf{x}_{i,j}(\mathbf{M}^*)) + n_{i,j}$. The decoding cost for \mathbf{M}^* is

$$\mathcal{D}(\mathbf{M}^*) \triangleq \sum_{i=1}^{n/k} \sum_{j=1}^{\ell_i} |y_{i,j} - h_{i,j} \mathbf{f}(\mathbf{x}_{i,j}(\mathbf{M}^*))|^2 = \sum_{i=1}^{n/k} \sum_{j=1}^{\ell_i} |n_{i,j}|^2. \quad (20)$$

The decoding cost of a wrong decoding sequences \mathbf{M}' is

$$\mathcal{D}(\mathbf{M}') \triangleq \sum_{i=1}^{n/k} \sum_{j=1}^{\ell_i} |y_{i,j} - h_{i,j} \mathbf{f}(\mathbf{x}_{i,j}(\mathbf{M}'))|^2. \quad (21)$$

Let \mathcal{E}_a be the event that there exists an error in the a^{th} segment, i.e., $\widehat{\mathbf{m}}_a \neq \mathbf{m}_a^*$. Denote $\bar{\mathcal{E}}_a$ as the complement of \mathcal{E}_a . The BLER of Spinal codes is expressed as:

$$\begin{aligned} P_e &\triangleq \Pr(\widehat{\mathbf{M}} \neq \mathbf{M}^*) = \Pr\left(\bigcup_{a=1}^{n/k} \mathcal{E}_a\right) = 1 - \Pr\left(\bigcap_{a=1}^{n/k} \bar{\mathcal{E}}_a\right) \\ &= 1 - \prod_{a=1}^{n/k} \left[1 - \Pr\left(\mathcal{E}_a \middle| \bigcap_{i=1}^{a-1} \bar{\mathcal{E}}_i\right) \right]. \end{aligned} \quad (22)$$

The next step is to calculate the conditional probability $\Pr(\mathcal{E}_a | \bigcap_{i=1}^{a-1} \bar{\mathcal{E}}_i)$. We define $\mathcal{W}_a \triangleq \{(\mathbf{m}'_1, \dots, \mathbf{m}'_a) : \mathbf{m}'_1 = \mathbf{m}_1^*, \dots, \mathbf{m}'_{a-1} = \mathbf{m}_{a-1}^*, \mathbf{m}'_a \neq \mathbf{m}_a^*\} \subseteq \mathcal{W}$, capturing sequences matching the correct sequence in the first $a-1$ segments but differing in the a -th. The conditional probability thus reflects the chance of any sequence in \mathcal{W}_a having a lower decoding cost than \mathbf{M}^* :

$$\Pr\left(\mathcal{E}_a \middle| \bigcap_{i=1}^{a-1} \bar{\mathcal{E}}_i\right) = \Pr(\exists \mathbf{M}' \in \mathcal{W}_a : \mathcal{D}(\mathbf{M}') \leq \mathcal{D}(\mathbf{M}^*)). \quad (23)$$

Applying the union bound of probability yields

$$\Pr\left(\mathcal{E}_a \middle| \bigcap_{i=1}^{a-1} \bar{\mathcal{E}}_i\right) \leq \min \left\{ 1, \sum_{\mathbf{M}' \in \mathcal{W}_a} \Pr(\mathcal{D}(\mathbf{M}') \leq \mathcal{D}(\mathbf{M}^*)) \right\}. \quad (24)$$

Then, substituting (20) and (21) into $\Pr(\mathcal{D}(\mathbf{M}') \leq \mathcal{D}(\mathbf{M}^*))$ in (24), the probability $\Pr(\mathcal{D}(\mathbf{M}') \leq \mathcal{D}(\mathbf{M}^*))$ turns to

$$\begin{aligned} &\Pr\left(\sum_{i=1}^{n/k} \sum_{j=1}^{\ell_i} |y_{i,j} - h_{i,j} \mathbf{f}(\mathbf{x}_{i,j}(\mathbf{M}'))|^2 \leq \sum_{i=1}^{n/k} \sum_{j=1}^{\ell_i} |n_{i,j}|^2\right) \\ &\stackrel{(a)}{=} \Pr\left(\sum_{i=a}^{n/k} \sum_{j=1}^{\ell_i} |y_{i,j} - h_{i,j} \mathbf{f}(\mathbf{x}_{i,j}(\mathbf{M}'))|^2 \leq \sum_{i=a}^{n/k} \sum_{j=1}^{\ell_i} |n_{i,j}|^2\right), \end{aligned} \quad (25)$$

where (a) establishes since $\mathbf{f}(\mathbf{x}_{i,j}(\mathbf{M}^*)) = \mathbf{f}(\mathbf{x}_{i,j}(\mathbf{M}'))$ for $1 \leq i < a$, which is proved in Appendix A by leveraging the properties of the hash function. Then, substituting $y_{i,j} =$

$h_{i,j} f(\mathbf{x}_{i,j}(\mathbf{M}^*)) + n_{i,j}$ into the RHS of (25) and introducing a complex variable $V_{i,j} = h_{i,j}(f(\mathbf{x}_{i,j}(\mathbf{M}^*)) - f(\mathbf{x}_{i,j}(\mathbf{M}')))$ $\in \mathbb{C}$ transforms the RHS of (25) into

$$\Pr\left(\sum_{i=a}^{n/k} \sum_{j=1}^{\ell_i} |V_{i,j} + n_{i,j}|^2 \leq \sum_{i=a}^{n/k} \sum_{j=1}^{\ell_i} |n_{i,j}|^2\right). \quad (26)$$

Note that

$$|V_{i,j} + n_{i,j}|^2 = |V_{i,j}|^2 + V_{i,j}n_{i,j}^* + V_{i,j}^*n_{i,j} + |n_{i,j}|^2, \quad (27)$$

(26) could be transformed into a simplified form as:

$$\Pr\left(\sum_{i=a}^{n/k} \sum_{j=1}^{\ell_i} |V_{i,j}|^2 + \sum_{i=a}^{n/k} \sum_{j=1}^{\ell_i} (V_{i,j}n_{i,j}^* + V_{i,j}^*n_{i,j}) \leq 0\right). \quad (28)$$

Solving (28) is still not straightforward, we are thus motivated to further simplify it. Let $\mathbf{V}^{L_a} \in \mathbb{C}^{L_a}$ be the row vector composed of the complex random variables $\{V_{i,j}\}_{i \in [n/k], j \in [\ell_i]}$, and let $\mathbf{N}^{L_a} \in \mathbb{C}^{L_a}$ be the row vector composed of the complex random variables $\{n_{i,j}\}_{i \in [n/k], j \in [\ell_i]}$. Then, (28) can be rewritten as:

$$\Pr\left(\Re\left[\mathbf{V}^{L_a}(\mathbf{V}^{L_a} + 2\mathbf{N}^{L_a})^H\right] \leq 0\right). \quad (29)$$

Expanding (29) yields (30) at this page's bottom. To solve (30), we first evaluate $\Pr(\Re[\mathbf{v}^{L_a}(\mathbf{v}^{L_a} + 2\mathbf{N}^{L_a})^H] \leq 0)$ and $\Pr(\mathbf{V}^{L_a} = \mathbf{v}^{L_a})$. We begin with simplifying the first probability using an upcoming lemma.

Lemma 2. *Given that $n_{i,j}$ is i.i.d complex AWGN with variance σ^2 , i.e., $n_{i,j} \sim \mathcal{CN}(0, \sigma^2)$, the probability $\Pr(\Re[\mathbf{v}^{L_a}(\mathbf{v}^{L_a} + 2\mathbf{N}^{L_a})^H] \leq 0)$ can be expressed as:*

$$\Pr\left(\Re\left[\mathbf{v}^{L_a}(\mathbf{v}^{L_a} + 2\mathbf{N}^{L_a})^H\right] \leq 0\right) = Q\left(\frac{\|\mathbf{v}^{L_a}\|_2}{\sqrt{2}\sigma}\right). \quad (31)$$

Proof. Solving $\Pr\left(\Re\left[\mathbf{v}^{L_a}(\mathbf{v}^{L_a} + 2\mathbf{N}^{L_a})^H\right] \leq 0\right)$ is challenging due to the high dimensionality of \mathbf{v}^{L_a} and \mathbf{N}^{L_a} . To simplify, we introduce an $L_a \times L_a$ unitary matrix \mathbf{A} to rotate these vectors into a lower-dimensional space. \mathbf{A} , defined in $\mathbb{C}^{L_a \times L_a}$, satisfies the unitary condition $\mathbf{A}^H \mathbf{A} = \mathbf{I}_{L_a}$. Without loss of generality, we assume \mathbf{A} satisfies that

$$\mathbf{A}[\mathbf{v}^{L_a}]^H = \left[\|\mathbf{v}^{L_a}\|_2, \underbrace{0, \dots, 0}_{L_a-1}\right]^T, \quad (32)$$

which indicates that the unitary matrix \mathbf{A} rotates the vector \mathbf{v}^{L_a} to the direction of a standard basis. Leveraging $\mathbf{A}^H \mathbf{A} = \mathbf{I}_{L_a}$, the probability of interest $\Pr\left(\Re\left[\mathbf{v}^{L_a}(\mathbf{v}^{L_a} + 2\mathbf{N}^{L_a})^H\right] \leq 0\right)$ can be transformed as:

$$\Pr\left(\Re\left[\mathbf{v}^{L_a} \mathbf{I}_{L_a}(\mathbf{v}^{L_a} + 2\mathbf{N}^{L_a})^H\right] \leq 0\right)$$

$$\begin{aligned} &= \Pr\left(\Re\left[\mathbf{v}^{L_a} \mathbf{A}^H \mathbf{A}(\mathbf{v}^{L_a} + 2\mathbf{N}^{L_a})^H\right] \leq 0\right) \\ &= \Pr\left(\Re\left\{\left[\mathbf{A}[\mathbf{v}^{L_a}]^H\right]^H \left(\mathbf{A}[\mathbf{v}^{L_a}]^H + 2\mathbf{A}[\mathbf{N}^{L_a}]^H\right)\right\} \leq 0\right). \end{aligned} \quad (33)$$

Substitute (32) into the RHS of (33), we have

$$\begin{aligned} &\Pr\left(\Re\left\{\|\mathbf{v}^{L_a}\|^2 + 2\|\mathbf{v}^{L_a}\|_2 \cdot \mathbf{A}_1[\mathbf{N}^{L_a}]^H\right\} \leq 0\right) \\ &= \Pr\left(\Re\left\{\mathbf{A}_1[\mathbf{N}^{L_a}]^H\right\} \leq -\frac{\|\mathbf{v}^{L_a}\|_2}{2}\right). \end{aligned} \quad (34)$$

To simplify the RHS of (34), we next introduce another tool, named the isotropic properties of random vectors.

Lemma 3. [36, A. 26, Page 502]. *If $\mathbf{w} \sim \mathcal{CN}(0, \sigma^2 \mathbf{I}_{L_a})$, then \mathbf{w} is isotropic, i.e., $\mathbf{U}[\mathbf{N}^{L_a}]^H \sim [\mathbf{N}^{L_a}]^H$ for any unitary matrix $\mathbf{U} \in \mathbb{C}^{L_a \times L_a}$.*

Corollary 3. $\mathbf{A}_1[\mathbf{N}^{L_a}]^H \sim \mathcal{CN}(0, \sigma^2)$.

Proof. As $[\mathbf{N}^{L_a}]^H \sim \mathcal{CN}(0, \sigma^2 \mathbf{I}_{L_a})$ and \mathbf{A} is the unitary matrix, it holds from Lemma 3 that $\mathbf{A}[\mathbf{N}^{L_a}]^H \sim [\mathbf{N}^{L_a}]^H \sim \mathcal{CN}(0, \sigma^2 \mathbf{I}_{L_a})$. Since \mathbf{A}_1 is the first row of the unitary matrix \mathbf{A} , the product $\mathbf{A}_1[\mathbf{N}^{L_a}]^H$ is also the first row of $\mathbf{A}[\mathbf{N}^{L_a}]^H$, following the distribution $\mathcal{CN}(0, \sigma^2)$. \square

Since $\mathbf{A}_1[\mathbf{N}^{L_a}]^H \sim \mathcal{CN}(0, \sigma^2)$, we could rewrite $\mathbf{A}_1[\mathbf{N}^{L_a}]^H$ as $\mathbf{A}_1[\mathbf{N}^{L_a}]^H = W_R + jW_I$, with $W_R, W_I \sim \mathcal{N}(0, \sigma^2/2)$. Therefore, the RHS of (34) can be further simplified by:

$$\Pr\left(W_R \leq -\frac{\|\mathbf{v}^{L_a}\|_2}{2}\right) = Q\left(\frac{\|\mathbf{v}^{L_a}\|_2}{\sqrt{2}\sigma}\right). \quad (35)$$

We thus accomplish the proof of Lemma 2. \square

With Lemma 2 in hand, (30) is extremely simplified:

$$\iint_{\mathbb{C}^{L_a}} Q\left(\frac{\|\mathbf{v}^{L_a}\|_2}{\sqrt{2}\sigma}\right) \cdot \Pr(\mathbf{V}^{L_a} = \mathbf{v}^{L_a}) \, d\mathbf{v}^{L_a}. \quad (36)$$

However, explicitly solving (36) is still challenging. The presence of the Q function within the integral adds to the complexity of this solution. To overcome this difficulty, we resort to a novel transformation of the Q function, referred to as Craig's formula [37]:

$$Q(x) = \frac{1}{\pi} \int_0^{\frac{\pi}{2}} \exp\left(\frac{-x^2}{2\sin^2\theta}\right) d\theta, \quad (37)$$

This transformation repositions the variables of the Q function from the integral's lower limits to the integrand, thereby

$$\begin{aligned} \Pr\left(\Re\left[\mathbf{V}^{L_a}(\mathbf{V}^{L_a} + 2\mathbf{N}^{L_a})^H\right] \leq 0\right) &= \iint_{\mathbb{C}^{L_a}} \Pr\left(\Re\left[\mathbf{V}^{L_a}(\mathbf{V}^{L_a} + 2\mathbf{N}^{L_a})^H\right] \leq 0 \mid \mathbf{V}^{L_a} = \mathbf{v}^{L_a}\right) \cdot \Pr(\mathbf{V}^{L_a} = \mathbf{v}^{L_a}) \, d\mathbf{v}^{L_a} \\ &= \iint_{\mathbb{C}^{L_a}} \Pr\left(\Re\left[\mathbf{v}^{L_a}(\mathbf{v}^{L_a} + 2\mathbf{N}^{L_a})^H\right] \leq 0\right) \cdot \Pr(\mathbf{V}^{L_a} = \mathbf{v}^{L_a}) \, d\mathbf{v}^{L_a}, \end{aligned} \quad (30)$$

$$\sum_{\beta_i, \beta_j \in \Psi} \mathbb{P}_{f(\mathbf{x}_{a,1}(\mathbf{M}'))}(\beta_i) \mathbb{P}_{f(\mathbf{x}_{a,1}(\mathbf{M}^*))}(\beta_j) \mathbb{E}_H \left[\exp \left\{ -\frac{|H(\beta_i - \beta_j)|^2}{4\sigma^2 \sin^2 \theta} \right\} \right] = \sum_{\beta_i, \beta_j \in \Psi} 2^{-2c} \mathbb{E}_H \left[\exp \left\{ -\frac{|H(\beta_i - \beta_j)|^2}{4\sigma^2 \sin^2 \theta} \right\} \right] \quad (43)$$

simplifying the analysis. By leveraging the *Craig's formula* and interchanging the integrals, (36) is transformed as

$$\frac{1}{\pi} \int_0^{\frac{\pi}{2}} \iint_{\mathcal{C}^{L_a}} \exp \left\{ \frac{-\|\mathbf{v}^{L_a}\|_2^2}{4\sigma^2 \sin^2 \theta} \right\} \cdot \Pr(\mathbf{V}^{L_a} = \mathbf{v}^{L_a}) \, d\mathbf{v}^{L_a} d\theta, \quad (38)$$

where $\Pr(\mathbf{V}^{L_a} = \mathbf{v}^{L_a})$ is given by adopting the i.i.d of $V_{i,j}$ (see Appendix C for the proof):

$$\Pr(\mathbf{V}^{L_a} = \mathbf{v}^{L_a}) = \prod_{i=a}^{n/k} \prod_{j=1}^{\ell_i} f_{V_{i,j}}(v_{i,j}), \quad (39)$$

Upon substituting (39) into (38), the internal integrals of (38) with respect to (w.r.t) \mathbf{v}^{L_a} could be decomposed

$$\begin{aligned} & \iint_{\mathcal{C}^{L_a}} \exp \left\{ \frac{-\|\mathbf{v}^{L_a}\|_2^2}{4\sigma^2 \sin^2 \theta} \right\} \cdot \Pr(\mathbf{V}^{L_a} = \mathbf{v}^{L_a}) \, d\mathbf{v}^{L_a} \\ & \stackrel{(a)}{=} \prod_{i=a}^{n/k} \prod_{j=1}^{\ell_i} \iint_{\mathcal{C}} \exp \left\{ \frac{-|v_{i,j}|^2}{4\sigma^2 \sin^2 \theta} \right\} f_{V_{i,j}}(v_{i,j}) \, dv_{i,j} \\ & \stackrel{(b)}{=} \left(\iint_{\mathcal{C}} \exp \left\{ -\frac{|v_{a,1}|^2}{4\sigma^2 \sin^2 \theta} \right\} f_{V_{a,1}}(v_{a,1}) \, dv_{a,1} \right)^{L_a} \\ & \stackrel{(c)}{=} \left(\mathbb{E}_{V_{a,1}} \left[\exp \left\{ -\frac{|V_{a,1}|^2}{4\sigma^2 \sin^2 \theta} \right\} \right] \right)^{L_a}, \end{aligned} \quad (40)$$

where (a) is obtained by expanding

$$\exp \left\{ \frac{-\|\mathbf{v}^{L_a}\|_2^2}{4\sigma^2 \sin^2 \theta} \right\} = \prod_{i=a}^{n/k} \prod_{j=1}^{\ell_i} \exp \left\{ \frac{-v_{i,j}^2}{4\sigma^2 \sin^2 \theta} \right\} \quad (41)$$

and interchanging the prod and the integral, (b) is due the the i.i.d of $V_{i,j}$ (see Appendix C for the proof), and (c) is established according to the definition of expectation.

Note that $V_{a,1} = h_{a,1}(f(\mathbf{x}_{a,1}(\mathbf{M}^*)) - f(\mathbf{x}_{a,1}(\mathbf{M}')))$, the expectation $\mathbb{E}_{V_{a,1}} \left[\exp \left\{ -\frac{|V_{a,1}|^2}{4\sigma^2 \sin^2 \theta} \right\} \right]$ in the RHS of (40) can be expanded as

$$\mathbb{E}_{\substack{h_{a,1}, f(\mathbf{x}_{a,1}(\mathbf{M}')), \\ f(\mathbf{x}_{a,1}(\mathbf{M}^*))}} \left[\exp \left\{ -\frac{|h_{a,1}(f(\mathbf{x}_{a,1}(\mathbf{M}^*)) - f(\mathbf{x}_{a,1}(\mathbf{M}')))|^2}{4\sigma^2 \sin^2 \theta} \right\} \right]. \quad (42)$$

Since the fading coefficient $h_{a,1}$, the encoded symbols $f(\mathbf{x}_{a,1}(\mathbf{M}'))$, and $f(\mathbf{x}_{a,1}(\mathbf{M}^*))$ are mutually independent (see Appendix C for the proof), (42) can be expanded as shown in equation (43) at the top of this page, and the integral in (38) turns to

$$\frac{1}{\pi} \int_0^{\frac{\pi}{2}} \left(\sum_{\beta_i, \beta_j \in \Psi} 2^{-2c} \mathbb{E}_H \left[\exp \left\{ -\frac{|H(\beta_i - \beta_j)|^2}{4\sigma^2 \sin^2 \theta} \right\} \right] \right)^{L_a} d\theta. \quad (44)$$

However, solving (44) is still a non-trivial work due to the exponential form of the integrand. In fact, there is no explicit

solution to the integral (44). As an alternative, we leverage the *Riemann sum* to address this issue. Specifically, we find that

Lemma 4. $\mathbb{E}_H \left[\exp \left\{ -\frac{|H(\beta_i - \beta_j)|^2}{4\sigma^2 \sin^2 \theta} \right\} \right]$ is monotonically increasing with θ .

With Lemma 4 in hand, we could leverage the *rule of right Riemann sum* to tightly upper bound the integral. Specifically, we can choose $N + 1$ values of θ such that $\theta_0 = 0$, $\theta_N = \frac{\pi}{2}$ and $0 < \theta_1 < \theta_2 < \dots < \theta_{N-1} < \frac{\pi}{2}$ to partition the region of the integral field, and then upper bound the integral through the *rule of right Riemann sum*:

$$\begin{aligned} & \frac{1}{\pi} \int_0^{\frac{\pi}{2}} \left(\sum_{\beta_i, \beta_j \in \Psi} 2^{-2c} \mathbb{E}_H \left[\exp \left\{ -\frac{|H(\beta_i - \beta_j)|^2}{4\sigma^2 \sin^2 \theta} \right\} \right] \right)^{L_a} d\theta \\ & = \frac{1}{\pi} \sum_{t \in [N]} \int_{\theta_{t-1}}^{\theta_t} \left(\sum_{\beta_i, \beta_j \in \Psi} 2^{-2c} \mathbb{E}_H \left[\exp \left\{ -\frac{|H(\beta_i - \beta_j)|^2}{4\sigma^2 \sin^2 \theta} \right\} \right] \right)^{L_a} d\theta \\ & \leq \sum_{t \in [N]} b_t \left(\sum_{\beta_i, \beta_j \in \Psi} 2^{-2c} \mathbb{E}_H \left[\exp \left\{ -\frac{|H(\beta_i - \beta_j)|^2}{4\sigma^2 \sin^2 \theta_t} \right\} \right] \right)^{L_a}, \end{aligned} \quad (45)$$

where $b_t = \frac{\theta_t - \theta_{t-1}}{\pi}$. Denote the RHS of (45) as $\mathcal{F}(L_a, \sigma)$ and substitute it back into (24), we have that

$$\sum_{\mathbf{M}' \in \mathcal{W}_a} \Pr(\mathcal{D}(\mathbf{M}') \leq \mathcal{D}(\mathbf{M})) \leq |\mathcal{W}_a| \cdot \mathcal{F}(L_a, \sigma), \quad (46)$$

where $|\mathcal{W}_a| = (2^k - 1)2^{n-ak}$. Substituting (46) into (23) and (24) and denote the RHS of (24) as ϵ_a , we obtain the bound. \square

V. DISCUSSIONS AND CASE STUDIES

This section discusses some significant insights obtained through the derived bounds.

A. Existence of the Bound

The central approach for deriving an explicit bound for Spinal codes involves calculating the expectation $\mathbb{E}_H \left[\exp \left\{ -\frac{|H(\beta_i - \beta_j)|^2}{4\sigma^2 \sin^2 \theta_t} \right\} \right]$. A preliminary step in this process is to prove that this expectation remains bounded under any fading coefficient H distribution, thereby ensuring the existence of the proposed bound.

Lemma 5. $\mathbb{E}_H \left[\exp \left\{ \frac{-|H(\beta_i - \beta_j)|^2}{4\sigma^2 \sin^2 \theta_t} \right\} \right]$ is always bounded, with $0 < \mathbb{E}_H \left[\exp \left\{ \frac{-|H(\beta_i - \beta_j)|^2}{4\sigma^2 \sin^2 \theta_t} \right\} \right] \leq 1$.

Proof. The lower bound of $\mathbb{E}_H \left[\exp \left\{ \frac{-|H(\beta_i - \beta_j)|^2}{4\sigma^2 \sin^2 \theta_t} \right\} \right]$ is 0, a fact that is straightforward to verify. Our focus is to prove that expectation does not exceed 1. Given that $|H(\beta_i - \beta_j)|^2 \geq 0$, we have $\exp \left\{ \frac{-|H(\beta_i - \beta_j)|^2}{4\sigma^2 \sin^2 \theta_t} \right\} \leq 1$. Then, applying the inequality $\mathbb{E}_X(f(X)) \leq \max f(X)$ infers that $\mathbb{E}_H \left[\exp \left\{ \frac{-|H(\beta_i - \beta_j)|^2}{4\sigma^2 \sin^2 \theta_t} \right\} \right] \leq 1$. \square

B. Properties of the Bound

This subsection further explores the properties of the bound. We find the following significant corollary to simplify the obtained bound.

Corollary 4. *The bound on BLER of Spinal codes correlates solely with the magnitude of the fading coefficient, and is independent of the phase.*

Proof. The proof is accomplished by

$$\begin{aligned} \mathbb{E}_H \left[\exp \left\{ \frac{-|H(\beta_i - \beta_j)|^2}{4\sigma^2 \sin^2 \theta_t} \right\} \right] &= \mathbb{E}_{R,\alpha} \left[\exp \left\{ \frac{-|Re^{j\alpha}(\beta_i - \beta_j)|^2}{4\sigma^2 \sin^2 \theta_t} \right\} \right] = \\ \mathbb{E}_{R,\alpha} \left[\exp \left\{ \frac{-R^2 |\beta_i - \beta_j|^2}{4\sigma^2 \sin^2 \theta_t} \right\} \right] &= \mathbb{E}_R \left[\exp \left\{ \frac{-R^2 |\beta_i - \beta_j|^2}{4\sigma^2 \sin^2 \theta_t} \right\} \right]. \end{aligned} \quad (47)$$

Thus, determining $\mathbb{E}_H \left[\exp \left\{ \frac{-|H(\beta_i - \beta_j)|^2}{4\sigma^2 \sin^2 \theta_t} \right\} \right]$ is equivalent to calculating $\mathbb{E}_R \left[\exp \left\{ \frac{-R^2 |\beta_i - \beta_j|^2}{4\sigma^2 \sin^2 \theta_t} \right\} \right]$ with respect to the fading modulus.

C. Case Studies over Specific Complex Fading Channels

In this subsection, we exemplify three case studies of **Theorem 2** by identifying the expectation $\mathbb{E}_R \left[\exp \left\{ \frac{-|R(\beta_i - \beta_j)|^2}{4\sigma^2 \sin^2 \theta_t} \right\} \right]$ in the RHS of (47). Over complex Rayleigh, Nakagami- m , and Rician fading channels, respectively. Upper bounds are explicitly derived.

1) Case Study 1: Complex Rayleigh Fading Channel

Corollary 5. *(Complex Rayleigh Fading Channel). Consider $(n, k, c, \Psi, v \gg 0)$ Spinal codes transmitted over a flat fast complex Rayleigh fading channel with mean square Ω and AWGN variance σ^2 , the average BLER given perfect CSI under ML decoding for Spinal codes can be upper bounded by **Theorem 2**, with the expectation $\mathbb{E}_R \left[\exp \left\{ \frac{-R^2 |\beta_i - \beta_j|^2}{4\sigma^2 \sin^2 \theta_t} \right\} \right]$ explicitly given by:*

$$\frac{4\sigma^2 \sin^2 \theta_t}{\Omega |\beta_i - \beta_j|^2 + 4\sigma^2 \sin^2 \theta_t}. \quad (48)$$

Proof. Over the Rayleigh fading channel, we have that the PDF of the modulus of $h_{i,j}$, denoted by R , is $f_R(r) = 2r/\Omega \cdot \exp\{-r^2/\Omega\}$. Thus, the expectation $\mathbb{E}_R \left[\exp \left\{ \frac{-R^2 |\beta_i - \beta_j|^2}{4\sigma^2 \sin^2 \theta_t} \right\} \right]$ could be expanded as:

$$\int_0^\infty \exp \left\{ \frac{-r^2 |\beta_i - \beta_j|^2}{4\sigma^2 \sin^2 \theta_t} \right\} \frac{2r}{\Omega} \exp \left(\frac{-r^2}{\Omega} \right) dr. \quad (49)$$

This integral, characterized by an infinite upper limit, is improper. However, it can be explicitly solved by

$$\begin{aligned} \frac{1}{\Omega} \int_0^\infty \exp \left\{ - \left(\frac{|\beta_i - \beta_j|^2}{4\sigma^2 \sin^2 \theta_t} + \frac{1}{\Omega} \right) r^2 \right\} dr^2 \\ = \frac{\exp \left\{ - \left(\frac{|\beta_i - \beta_j|^2}{4\sigma^2 \sin^2 \theta_t} + \frac{1}{\Omega} \right) r^2 \right\} \Big|_0^\infty}{-\Omega \left(\frac{|\beta_i - \beta_j|^2}{4\sigma^2 \sin^2 \theta_t} + \frac{1}{\Omega} \right)} = \frac{4\sigma^2 \sin^2 \theta_t}{\Omega |\beta_i - \beta_j|^2 + 4\sigma^2 \sin^2 \theta_t}. \end{aligned} \quad (50)$$

With (50) in hand, it is then straightforward to obtain the **Corollary 5** by substituting (50) into (18). \square

2) Case Study 2: Complex Nakagami- m Fading Channel

Corollary 6. *(Complex Nakagami- m Fading Channel). Consider $(n, k, c, \Psi, v \gg 0)$ Spinal codes transmitted over a flat fast complex Nakagami- m fading channel with mean square Ω , AWGN variance σ^2 , and Nakagami parameter m , the average BLER given perfect CSI under ML decoding for Spinal codes can be upper bounded by **Theorem 2**, with the expectation $\mathbb{E}_R \left[\exp \left\{ \frac{-R^2 |\beta_i - \beta_j|^2}{4\sigma^2 \sin^2 \theta_t} \right\} \right]$ explicitly given by:*

$$\left(\frac{4m\sigma^2 \sin^2 \theta_t}{\Omega |\beta_i - \beta_j|^2 + 4m\sigma^2 \sin^2 \theta_t} \right)^m. \quad (51)$$

Proof. Over the Nakagami- m fading channel, we have that the PDF of the modulus of $h_{i,j}$, denoted by R , is $f_R(r) = \frac{2m^m}{\Gamma(m)\Omega^m} \cdot r^{2m-1} \cdot \exp\{-mr^2/\Omega\}$. Thus, the expectation $\mathbb{E}_R \left[\exp \left\{ \frac{-R^2 |\beta_i - \beta_j|^2}{4\sigma^2 \sin^2 \theta_t} \right\} \right]$ could be expanded as:

$$\int_0^\infty \exp \left\{ \frac{-r^2 |\beta_i - \beta_j|^2}{4\sigma^2 \sin^2 \theta_t} \right\} \frac{2m^m}{\Gamma(m)\Omega^m} r^{2m-1} \exp \left\{ \frac{-mr^2}{\Omega} \right\} dr. \quad (52)$$

The remaining issue is to explicitly solve the above improper integral. This is achieved by carrying out the substitution $z = \frac{|\beta_i - \beta_j|^2}{4\sigma^2 \sin^2 \theta_t}$ into (52). Consequently, (52) turns to

$$\int_0^\infty \exp \left\{ - \left(z + \frac{m}{\Omega} \right) r^2 \right\} \cdot \frac{2m^m}{\Gamma(m)\Omega^m} r^{2m-1} dr. \quad (53)$$

Performing the variable substitution $t = \left(z + \frac{m}{\Omega} \right) r^2$ and (53) turns to

$$\frac{m^m}{\Gamma(m)(z\Omega + m)^m} \underbrace{\int_0^\infty e^{-t} t^{m-1} dt}_{\Gamma(m)} = \frac{m^m}{(z\Omega + m)^m}. \quad (54)$$

Thus, applying $z = \frac{|\beta_i - \beta_j|^2}{4\sigma^2 \sin^2 \theta_t}$ back in (54) and we have (51). \square

Remark 2. *Corollary 6 also represents as an extension of Corollary 5. If $m = 1$, the equation (51) reduces to (48), and the Nakagami- m fading reduces to the Rayleigh fading.*

Lemma 6. *When $m \rightarrow \infty$, (51) turns to*

$$\lim_{m \rightarrow \infty} \left(\frac{4m\sigma^2 \sin^2 \theta_t}{\Omega |\beta_i - \beta_j|^2 + 4m\sigma^2 \sin^2 \theta_t} \right)^m = \exp \left\{ - \frac{\Omega |\beta_i - \beta_j|^2}{4\sigma^2 \sin^2 \theta_t} \right\}. \quad (55)$$

Proof. This limit can be attained by utilizing the fundamental limit expression $\lim_{x \rightarrow \infty} (1 - 1/x)^x = e^{-1}$. \square

Remark 3. *In case of Lemma 6, the fading of the Nakagami- m channel could be neglected and the channel turns to an AWGN channel if the mean square of the fading $\Omega = 1$. Following the limit (55) with substitution $\Omega = 1$, we could obtain the upper bound on the BLER of Spinal codes over the AWGN channel.*

Lemma 7. *The function $F(m) = \left(\frac{4m\sigma^2 \sin^2 \theta_t}{\Omega |\beta_i - \beta_j|^2 + 4m\sigma^2 \sin^2 \theta_t} \right)^m$ is monotonically decreasing with m .*

Proof. To analyze $F(m)$, we apply logarithmic on it, as

$$\ln F(m) = m \ln \left(\frac{4m\sigma^2 \sin^2 \theta_t}{\Omega |\beta_i - \beta_j|^2 + 4m\sigma^2 \sin^2 \theta_t} \right), \quad (56)$$

$$\frac{d \ln F(m)}{dm} = \ln \left(1 - \frac{\Omega |\beta_i - \beta_j|^2}{\Omega |\beta_i - \beta_j|^2 + 4m\sigma^2 \sin^2 \theta_t} \right) + \frac{\Omega |\beta_i - \beta_j|^2}{\Omega |\beta_i - \beta_j|^2 + 4m\sigma^2 \sin^2 \theta_t} \quad (57)$$

whose derivation is shown in (57). It is noted that the inequality $f(x) = \ln(1-x) + x \leq 0$ is always valid for $x > 0$. Applying this to our context, we could obtain that $\frac{d \ln F(m)}{dm} = f \left(\frac{\Omega |\beta_i - \beta_j|^2}{\Omega |\beta_i - \beta_j|^2 + 4m\sigma^2 \sin^2 \theta_t} \right)$. Given the established inequality for $f(x)$, it follows that $\frac{d \ln F(m)}{dm} \leq 0$. This implies that $\ln F(m)$, and therefore $F(m)$ itself, is monotonically decreasing with respect to m . \square

Remark 4. From (17) and (18), it can be established that $\mathcal{F}(L_a, \sigma)$ is monotonically increasing with $F(m)$. Meanwhile, P_e is monotonically increasing with $\mathcal{F}(L_a, \sigma)$. Utilizing the chain rule for derivatives, we know the upper bound on the BLER of Spinal codes over the Nakagami- m fading channel is decreasing with the parameter m .

3) Case Study 3: Complex Rician Fading Channel

Corollary 7. (Complex Rician Fading Channel). Consider $(n, k, c, \Psi, v \gg 0)$ Spinal codes transmitted over a flat fast complex Rician fading channel with mean square Ω , AWGN variance σ^2 , and Rician factor K , the average BLER given perfect CSI under ML decoding for Spinal codes can be upper bounded by **Theorem 2**, with the expectation $\mathbb{E}_R \left[\exp \left\{ \frac{-R^2 |\beta_i - \beta_j|^2}{4\sigma^2 \sin^2 \theta_t} \right\} \right]$ explicitly given by:

$$f(K) = \frac{4(K+1)\sigma^2 \sin^2 \theta_t}{\Omega |\beta_i - \beta_j|^2 + 4(K+1)\sigma^2 \sin^2 \theta_t} \times \exp \left\{ \frac{-K\Omega |\beta_i - \beta_j|^2}{\Omega |\beta_i - \beta_j|^2 + 4(K+1)\sigma^2 \sin^2 \theta_t} \right\}. \quad (58)$$

Proof. Over the Rician fading channel, we have that the PDF of the modulus of $h_{i,j}$, denoted by R , is $f_R(r) = \frac{2(K+1)r}{\Omega \exp \left\{ K + \frac{(K+1)r^2}{\Omega} \right\}} I_0 \left(2\sqrt{\frac{K(K+1)}{\Omega}} r \right)$. Thus, the expectation $\mathbb{E}_R \left[\exp \left\{ \frac{-R^2 |\beta_i - \beta_j|^2}{4\sigma^2 \sin^2 \theta_t} \right\} \right]$ could be expanded as:

$$\int_0^\infty \exp \left\{ \frac{-r^2 |\beta_i - \beta_j|^2}{4\sigma^2 \sin^2 \theta_t} \right\} \frac{2(K+1)r}{\Omega \exp \left\{ K + \frac{(K+1)r^2}{\Omega} \right\}} I_0 \left(2\sqrt{\frac{K(K+1)}{\Omega}} r \right) dr. \quad (59)$$

The remaining challenge lies in explicitly solving the aforementioned improper integral. Intriguingly, this integral can be transformed into a succinct closed-form expression. To illustrate this, we first execute a substitution defined as $z = \frac{|\beta_i - \beta_j|^2}{4\sigma^2 \sin^2 \theta_t}$, which simplifies (59) as

$$\frac{2(K+1)}{\Omega e^K} \int_0^\infty r \exp \left\{ - \left(\frac{K+1}{\Omega} + z \right) r^2 \right\} I_0 \left(2\sqrt{\frac{K(K+1)}{\Omega}} r \right) dr. \quad (60)$$

The presence of the Bessel function $I_0(\cdot)$ complicates the subsequent analysis. However, it is noteworthy that the Bessel function can be expanded as an infinite series, expressed as

$$I_0(x) = \sum_{m=0}^{\infty} \frac{(-1)^m}{(m!)^2} \left(\frac{x}{2} \right)^{2m}. \quad (61)$$

Substituting the infinite series back into (60) yields

$$\frac{2}{e^K} \sum_{m=0}^{\infty} \frac{K^m (K+1)^{m+1}}{m! \Gamma(m+1) \Omega^{m+1}} \underbrace{\int_0^\infty r^{2m+1} \exp \left\{ - \left(\frac{K+1}{\Omega} + z \right) r^2 \right\} dr}_{\mathcal{J}}. \quad (62)$$

Let $t = \left(z + \frac{K+1}{\Omega} \right) r^2$, the integral inherent in (62), denoted as \mathcal{J} , can be explicitly solved as

$$\mathcal{J} = \frac{\int_0^\infty e^{-t} t^m dt}{2 \left(z + \frac{K+1}{\Omega} \right)^{m+1}} = \frac{\Gamma(m+1)}{2 \left(z + \frac{K+1}{\Omega} \right)^{m+1}}. \quad (63)$$

Then, substitute (63) into (62), we simplify the original improper integral to an infinite series:

$$\frac{1}{K e^K} \cdot \sum_{m=0}^{\infty} \frac{1}{m!} \left(\frac{K(K+1)}{\Omega z + K + 1} \right)^{m+1}. \quad (64)$$

By applying the infinite series over the exponential function $\exp\{x\} = \sum_{m=0}^{\infty} \frac{1}{m!} x^m$, we finally express (64) into a compact closed form, given as

$$\frac{K+1}{\Omega z + K + 1} \cdot \exp \left\{ \frac{-K\Omega z}{\Omega z + K + 1} \right\}. \quad (65)$$

Then, substituting $z = \frac{|u|^2}{4\sigma^2 \sin^2 \theta_t}$ back into (65) yields (58). \square

Remark 5. *Corollary 7* represents as an extension of *Corollary 5*. If $K = 0$, (58) reduces to (48), and the Rician fading reduces to the Rayleigh fading.

Lemma 8. When $K \rightarrow \infty$, we have the limit of (58) as follows

$$\lim_{K \rightarrow \infty} F(K) = \exp \left\{ - \frac{\Omega |\beta_i - \beta_j|^2}{4\sigma^2 \sin^2 \theta_t} \right\}. \quad (66)$$

Proof. Denote the first part of (58) as $F_1(K)$ and the second part as $F_2(K)$, with $F_1(K) = \frac{4(K+1)\sigma^2 \sin^2 \theta_t}{\Omega |\beta_i - \beta_j|^2 + 4(K+1)\sigma^2 \sin^2 \theta_t}$ and $F_2(K) = \exp \left\{ \frac{-K\Omega |\beta_i - \beta_j|^2}{\Omega |\beta_i - \beta_j|^2 + 4(K+1)\sigma^2 \sin^2 \theta_t} \right\}$, we have

$$\lim_{K \rightarrow \infty} F(K) = \lim_{K \rightarrow \infty} F_1(K) \cdot \lim_{K \rightarrow \infty} F_2(K), \quad (67)$$

with

$$\lim_{K \rightarrow \infty} F_1(K) = 1, \quad \lim_{K \rightarrow \infty} F_2(K) = \exp \left\{ - \frac{\Omega |\beta_i - \beta_j|^2}{4\sigma^2 \sin^2 \theta_t} \right\}. \quad (68)$$

Substituting (68) into (67) accomplishes the proof. \square

Remark 6. In case of **Lemma 8**, the LOS component dominates the channel, transforming the Rician channel into an AWGN channel if $\Omega = 1$. Following the limit (66) with substitution $\Omega = 1$, we could obtain the upper bound on the BLER of Spinal codes over the AWGN channel.

Lemma 9. $F(K)$ in (58) is monotonically decreasing with K .

Proof. Denote $a = \frac{\Omega|\beta_i - \beta_j|^2}{4\sigma^2 \sin^2 \theta_t}$, and we could rewrite (58) as

$$F(K) = \frac{K+1}{a+K+1} \cdot \exp\left\{\frac{-Ka}{a+K+1}\right\}. \quad (69)$$

The derivative of (69) is

$$\frac{dF(K)}{dK} = \frac{-[a^2 + (K+1)(a^2 + a + 1)]}{(a+K+1)^3} \cdot \exp\left\{\frac{-K\Omega z}{\Omega z + K + 1}\right\}. \quad (70)$$

As $a \geq 0$ and $K \geq 0$, we have $\frac{dF(K)}{dK} < 0$ straightforwardly. Thus, (58) is monotonically decreasing with K . \square

Remark 7. Given that $\mathcal{F}(L_a, \sigma)$ demonstrates a monotonic increase with $F(K)$, and similarly, P_e is monotonically increasing with $\mathcal{F}(L_a, \sigma)$, **Lemma 9** implies that the upper bound on the BLER of Spinal codes over the Rician fading channel is decreasing with the Rician factor K .

D. Real fading channel

Over the real fading channel with AWGN variance σ^2 , the applicability of the bound presented in **Theorem 2** necessitates a minor modification in terms of σ in (17). We present this modification upfront and leave the detailed discussion in the next section. This alteration involves converting $\mathcal{F}(L_a, \sigma)$ to $\mathcal{F}(L_a, \sqrt{2}\sigma)$, and (17) is adjusted to

$$\epsilon_a = \min\left\{1, (2^k - 1) 2^{n-ak} \cdot \mathcal{F}\left(L_a, \sqrt{2}\sigma\right)\right\}. \quad (71)$$

The key step in deriving explicit upper bounds on the BLER for Spinal codes in real fading channels involves computing $\mathcal{F}(L_a, \sqrt{2}\sigma)$ as

$$\sum_{t \in [N]} b_t \left(\sum_{\beta_i \in \Psi} \sum_{\beta_j \in \Psi} 2^{-2c} \mathbb{E}_R \left[\exp\left\{\frac{-R^2|\beta_i - \beta_j|^2}{8\sigma^2 \sin^2 \theta_t}\right\} \right] \right)^{L_a}, \quad (72)$$

which involves calculating $\mathbb{E}_R \left[\exp\left\{\frac{-R^2|\beta_i - \beta_j|^2}{8\sigma^2 \sin^2 \theta_t}\right\} \right]$. This is a unified result of our earlier work in [1, *Theorem 1-3*].

E. Tightness of the Bound

We explore the interrelation between **Theorem 2** and **Theorem 1** here. We theoretically prove that our proposed **Theorem 1** demonstrates greater tightness than **Theorem 1**.

Theorem 3. Under identical conditions of Spinal codes, fading distributions, and SNR, **Theorem 2** yields a more restrictive upper bound compared to **Theorem 1**.

Proof. For easy comparison, denote the ϵ_a in **Theorem 2** as $\epsilon_a^{(2)}$ and the ϵ_a in **Theorem 1** as $\epsilon_a^{(1)}$. The proof is equivalent to show that $\epsilon_a^{(2)} < \epsilon_a^{(1)}$. We first establish the following inequity

$$\mathcal{F}(L_a, \sigma) \leq \frac{1}{2} \left(\sum_{\beta_i, \beta_j \in \Psi} 2^{-2c} \mathbb{E}_H \left[\exp\left\{\frac{-|H(\beta_i - \beta_j)|^2}{4\sigma^2}\right\} \right] \right)^{L_a}, \quad (73)$$

where the proof is detailed in Appendix D. With (73) and (17), we know that

$$\epsilon_a^{(2)} \leq (2^k - 1) 2^{n-ak} \cdot \mathcal{F}(L_a, \sigma) \leq (2^k - 1) 2^{n-ak} \cdot \frac{1}{2} \left(\sum_{\beta_i, \beta_j \in \Psi} 2^{-2c} \mathbb{E}_H \left[\exp\left\{\frac{-|H(\beta_i - \beta_j)|^2}{4\sigma^2}\right\} \right] \right)^{L_a} \quad (74)$$

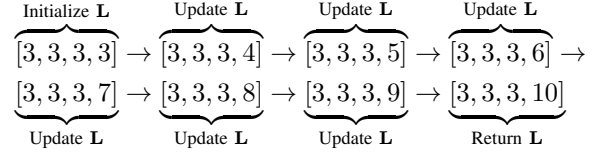


Fig. 2. A dynamic solution process of Algorithm 1. Parameter is set as $n = 8$, $k = 2$, $r = 3$, and $N = 19$.

Because $(2^k - 1)/2 < 2^k$ holds for $k > 0$, (74) turns to

$$\epsilon_a^{(2)} < 2^{n-ak+k} \cdot \left(\sum_{\beta_i, \beta_j \in \Psi} 2^{-2c} \mathbb{E}_H \left[\exp\left\{\frac{-|H(\beta_i - \beta_j)|^2}{4\sigma^2}\right\} \right] \right)^{L_a} = \epsilon_a^{(1)}. \quad (75)$$

VI. OPTIMAL TRANSMISSION SCHEME UNDER ML DECODING

This section aims at optimizing the transmission pattern scheme of Spinal codes. We formulate an BLER minimization problem constrained by a fixed coding rate and find that for ML-decoded Spinal codes, transmitting tail symbols consistently leads to the optimal solution. This theoretically supports the trick of transmitting tail symbols in the previous literature.

A. Problem Formulation and Solution

Leveraging the upper bound on the BLER of Spinal codes given in **Theorem 2**, denoted by P_e^U , we could establish an optimization problem to optimize Spinal codes' transmission. The optimization problem is explicitly given as:

$$\textbf{Problem 1.} \quad \min_{\mathbf{L}} P_e^U \quad \text{s.t.} \quad \sum_{i=1}^{n/k} \ell_i = N; \ell_i \in \mathbb{N}^+, i \in [n/k].$$

The above problem is an integer planning problem, which traditionally complex. To this end, we initially propose a greedy algorithm in **Algorithm 1** to derive a solution for **Problem 1**. The algorithm's dynamics, with parameters $r = 3$ and $N = 19$, are demonstrated in Fig. 2.

Algorithm 1: The greedy baseline algorithm for solving Problem 1

Input: Initialize number of transmitted passes p_{ini} ;
Preset the target number of pass N (make sure $p_{\text{ini}}n/k \leq N$);

Output: The number of symbols generated from each spine value $\mathbf{L} = [\ell_1, \ell_2, \dots, \ell_{n/k}]$;

- 1 Initialization: $\mathbf{L} = [p_{\text{ini}}, p_{\text{ini}}, \dots, p_{\text{ini}}]$, $N \geq p_{\text{ini}}n/k$;
 - 2 Calculate P_e^U by applying **Theorem 2**;
 - 3 **while** $\sum_{i=1}^{n/k} \ell_i < N$ **do**
 - 4 **for** $i \leftarrow 1$ to n/k **do**
 - 5 Update the decision variable: $\ell_i \leftarrow \ell_i + 1$;
 - 6 Calculate BLER bound $P_{e,i}^U$;
 - 7 Restore the decision variable: $\ell_i \leftarrow \ell_i - 1$;
 - 8 Search $d = \arg \min_i P_{e,i}^U$;
 - 9 Update $\ell_d \leftarrow \ell_d + 1$, $P_e^U \leftarrow P_{e,d}^U$;
 - 10 **return** \mathbf{L}
-

A distinct trend emerges in Fig. 2: the tail transmitting pattern (TTP), where iterations consistently transmit tail symbols. Subsequently, we'll offer a comprehensive proof validating TTP's optimality in ML-decoded Spinal codes.

B. Optimality of the TTP Scheme

It's important to note that while the TTP scheme's efficacy for Spinal codes was empirically identified in [4], a theoretical basis explaining its effectiveness remained unexplored. This work fills that gap by theoretically substantiating the TTP scheme's optimality.

Theorem 4. *The TTP scheme is optimal for Problem 1.*

Proof. We first examine the relationship between the BLER and code length given a fixed code rate.

Lemma 10. ϵ_a is non-increasing with L_a for $\forall 1 \leq a \leq n/k$.

Proof. Note that ϵ_a is non-increasing with $\mathcal{F}(L_a, \sigma)$, the monotony of ϵ_a w.r.t L_a is equivalent to the monotony of $\mathcal{F}(L_a, \sigma)$ w.r.t L_a . To discuss the monotony of $\mathcal{F}(L_a, \sigma)$ concerning L_a , it's essential to ascertain whether the base of the exponential function inherent in (18) exceeds 1. This base is defined as $\sum_{\beta_i \in \Psi} \sum_{\beta_j \in \Psi} 2^{-2c} \mathbb{E}_R \left[\exp \left\{ \frac{-R^2 |\beta_i - \beta_j|^2}{4\sigma^2 \sin^2 \theta_t} \right\} \right]$. Given that $\exp \left\{ \frac{-R^2 |\beta_i - \beta_j|^2}{4\sigma^2 \sin^2 \theta_t} \right\} \leq 1$, its expected value also holds that $\mathbb{E}_R \left[\exp \left\{ \frac{-R^2 |\beta_i - \beta_j|^2}{4\sigma^2 \sin^2 \theta_t} \right\} \right] \leq 1$. Consequently, we establish the following inequality:

$$\sum_{\beta_i \in \Psi} \sum_{\beta_j \in \Psi} 2^{-2c} \mathbb{E}_R \left[\exp \left\{ \frac{-R^2 |\beta_i - \beta_j|^2}{4\sigma^2 \sin^2 \theta_t} \right\} \right] \leq \sum_{\beta_i \in \Psi} \sum_{\beta_j \in \Psi} 2^{-2c} \leq 1, \quad (76)$$

which indicates that $\mathcal{F}(L_a, \sigma)$ is decreasing with L_a . Then, we obtain that ϵ_a is non-increasing with L_a . \square

With this **Lemma 10** in hand, we now start to prove the optimality of the TTP. Consider two types of transmission patterns, one is the TTP pattern, denoted by a vector

$$\mathbf{L}^* = (\ell_1, \ell_2, \dots, \ell_{n/k} + M), \quad (77)$$

where $(\ell_1, \ell_2, \dots, \ell_{n/k})$ is the initialization transmission pattern. The other could be arbitrary patterns, denoted by

$$\mathbf{L} = (\ell_1 + \delta_1, \ell_2 + \delta_2, \dots, \ell_{n/k} + \delta_{n/k}), \delta_i \in \mathbb{N}. \quad (78)$$

To ensure that both the aforementioned patterns align with the same code rate, they must satisfy that $\|\mathbf{L}^*\|_1 = \|\mathbf{L}\|_1$, which is equivalent to the condition $M = \sum_{j=1}^{n/k} \delta_j$. Subsequently, we compare the upper bounds on the BLER of Spinal codes with respect to \mathbf{L}^* and \mathbf{L} , respectively. Denote $P_e(\mathbf{L})$ and $P_e(\mathbf{L}^*)$ as the upper bounds on the BLER of ML-decoded Spinal codes w.r.t \mathbf{L} and \mathbf{L}^* . The optimality of the transmission pattern \mathbf{L}^* is equivalent to showing that its BLER, $P_e(\mathbf{L}^*)$, is the lowest when compared to the BLER, $P_e(\mathbf{L})$, of any other arbitrary patterns under the same code rate. This is mathematically described by the following **Proposition 1**. If we could prove that this proposition holds true, then we accomplish the proof of **Theorem 4**.

Proposition 1. *For $\forall M, \delta_1, \dots, \delta_{n/k} \in \mathbb{N}$ such that $M = \sum_{j=1}^{n/k} \delta_j$, $P_e(\mathbf{L}^*) \leq P_e(\mathbf{L})$.*

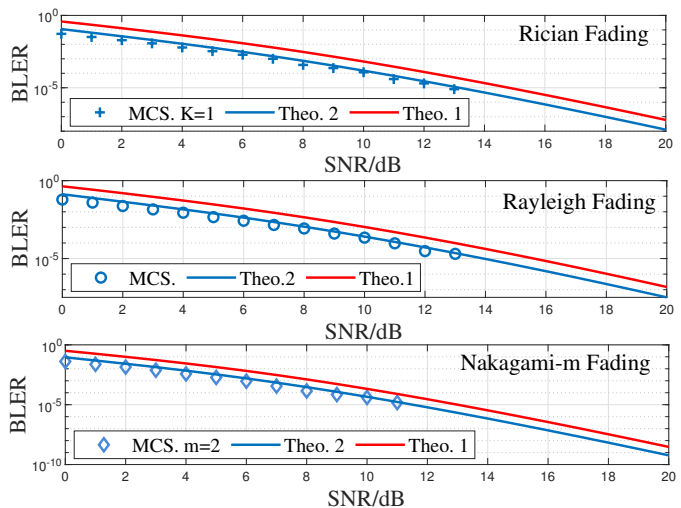


Fig. 3. Upper Bounds vs. Monte Carlo Simulations (MCS). BLER of Spinal codes with $n = 8, v = 32, pass = 6, c = 8$ and $k = 2$ over complex fading channels with $\Omega = 1$.

Proof. Performing (22) yields

$$P_e(\mathbf{L}) = 1 - \prod_{a=1}^{n/k} (1 - \epsilon_a(\mathbf{L})), P_e(\mathbf{L}^*) = 1 - \prod_{a=1}^{n/k} (1 - \epsilon_a(\mathbf{L}^*)). \quad (79)$$

Thus, it is natural to find that $\frac{\delta P_e}{\delta \epsilon_i} = \prod_{a \in [n/k]/i} (1 - \epsilon_a) \geq 0$ holds for $\forall i \in [n/k]$. This indicates that P_e is increasing with ϵ_i for $\forall i \in [n/k]$. Thus, we could initially explore the stronger inequalities such that $\epsilon_a(\mathbf{L}^*) \leq \epsilon_a(\mathbf{L})$ for $1 \leq a \leq n/k$. If these strong inequalities $\epsilon_a(\mathbf{L}^*) \leq \epsilon_a(\mathbf{L})$ for $1 \leq a \leq n/k$ hold true, then establishing the weaker inequality $P_e(\mathbf{L}^*) \leq P_e(\mathbf{L})$ becomes straightforward.

Fortunately, we can indeed prove that the strong inequalities $\epsilon_a(\mathbf{L}^*) \leq \epsilon_a(\mathbf{L})$ for $1 \leq a \leq n/k$ hold true. This is achieved by leveraging the monotonically decreasing nature of ϵ_a w.r.t L_a in **Lemma 10**. If we could prove $\mathbf{L}_a^* \geq \mathbf{L}_a$, where \mathbf{L}_a^* and \mathbf{L}_a are defined as the cumulative transmitted symbols after the a -th segment of Spinal codes, $\epsilon_a(\mathbf{L}^*) \leq \epsilon_a(\mathbf{L})$ naturally holds.

According to the definitions of \mathbf{L}_a^* and \mathbf{L}_a , together with (77) and (78), we have that

$$\mathbf{L}_a = \sum_{i=a}^{n/k} \ell_i + \sum_{i=a}^{n/k} \delta_i, \quad \mathbf{L}_a^* = M + \sum_{i=a}^{n/k} \ell_i. \quad (80)$$

Subtract \mathbf{L}_a from \mathbf{L}_a^* , we have

$$\mathbf{L}_a^* - \mathbf{L}_a = M - \sum_{i=a}^{n/k} \delta_i. \quad (81)$$

Note that $M = \sum_{i \in [n/k]} \delta_i$, we have $\mathbf{L}_a^* - \mathbf{L}_a = \sum_{i=1}^{a-1} \delta_i \geq 0$. With $\mathbf{L}_a^* \geq \mathbf{L}_a$, we could indicate by **Lemma 10** that $\epsilon_a(\mathbf{L}^*) \leq \epsilon_a(\mathbf{L})$, and thus accomplish the proof such that $P_e(\mathbf{L}^*) \leq P_e(\mathbf{L})$. \square

Now that **Proposition 1** holds true, we then accomplish the proof of **Theorem 4**. \square

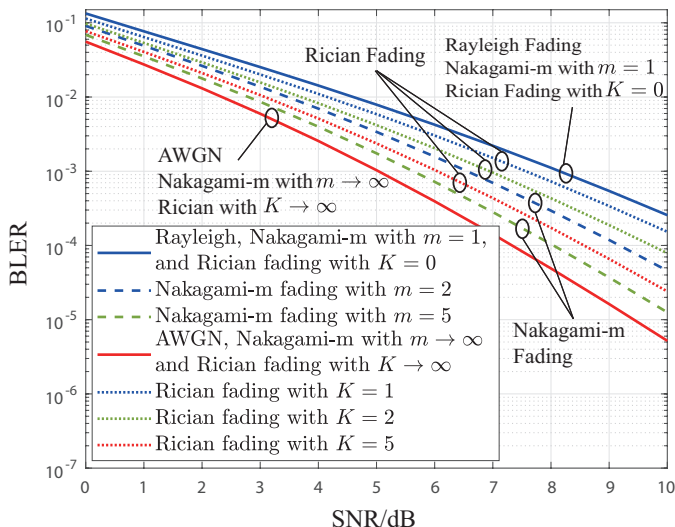


Fig. 4. Upper bounds under different parameters setup. Here $n = 8$, $v = 32$, $pass = 6$, $c = 8$, $k = 2$ and $\Omega = 1$. The upper bounds are obtained by **Theorem 2**.

VII. SIMULATIONS

In this section, we conduct simulations to verify the obtained bounds and to validate the insights.

A. Upper Bounds vs. Monte Carlo Simulations

Given the exponential complexity of ML-decoding, we opt for a relatively minimal value of $n = 8$ for the message size. We set the number of passes as $L = 6$ to facilitate a manageable ML-decoding Monte Carlo simulation setup. The parameter v is designated as $v = 32$, as substantiated by **Property 2** in Appendix A, elucidating that a hash collision is anticipated to occur once per 2^{32} hash function invocations on average. Additionally, we set $N = 20$ in **Corollary 5** to **Corollary 7** to ensure the precision of upper bounds approximations. The sample size for Monte Carlo simulations is set as 10^6 to calculate the average BLER. All channel mean square values are normalized by setting $\Omega = 1$. For complex Nakagami- m fading channels, the fading parameter is fixed at $m = 2$. For complex Rician fading channels, the Rician factor is set to $K = 1$.

Fig. 3 demonstrates that our derived bounds remain tight across a range of fading channels and SNR conditions. This illustrates our unified approach's robustness in providing tight BLER upper bounds for various fading scenarios. Notably, the approach in **Theorem 2** is tighter than that **Theorem 1**, which is based on the *Gallager bound*, consistent with our theoretical finding in **Theorem 3**.

B. Upper Bounds Under Different Parameters Setup

Fig. 4 illustrates various BLER upper bounds under different fading parameter settings. Some significant insights are discussed in the following.

1) Nakagami- m Fading Channel:

- *Overlap at $m = 1$ with Rayleigh Fading Channel.* The BLER upper bound for the Nakagami- m fading channel with $m = 1$ overlaps with that of the Rayleigh fading channel. This is because the Rayleigh fading channel will reduce to Nakagami-

m fading channel when $m = 1$, as discussed in **Remark 2**.

- *Convergence to AWGN Channel as m Approaches Infinity.* The convergence of the BLER upper bound to its infimum as m approaches infinity indicates the transition of the Nakagami- m fading channel towards an AWGN channel. This is consistent with that as m increases, the channel experiences less fading and approaches to an AWGN channel. This behavior is elaborated in **Remark 3**.

- *Decreasing Bound with Increasing m .* The trend of a decreasing BLER upper bound with increasing m values in the Nakagami- m fading channel, as seen in Fig. 4, aligns with the nature of the Nakagami- m model. This trend, confirmed in **Remark 4**, suggests that higher m values (indicating less severe fading) result in better channel conditions, leading to lower BLER.

2) Rician Fading Channel:

- *Overlap at $K = 0$ with Rayleigh Fading Channel.* The BLER upper bound for the Rician fading channel with $K = 0$ overlaps with that of the Rayleigh fading channel. This observation is consistent with **Remark 5**.

- *Convergence to AWGN Channel as K Approaches Infinity.* As K approaches infinity, indicating an increasingly dominant LOS signal component, the bound converges to its infimum, representing an ideal AWGN channel. This trend supports the insight in **Remark 6**.

- *Decreasing Bound as K Increases.* The regularity that the BLER upper bound decreases with increasing K supports that a stronger LOS signal component leads to improved channel conditions. This trend has been discussed in **Remark 7**.

VIII. CONCLUSION

This paper has derived two explicit upper bounds on the BLER of Spinal codes over real and complex fading channels. One bound is based on the variant of *Gallager bound*, the other bound customize Spinal codes better and has been proved to be tighter. Leveraging the obtained bound, we have obtained the TTP scheme have theoretically unveiled the optimality of the TTP for ML-decoded Spinal codes.

Prospective research avenues could extend to the theoretical BLER analysis of Spinal codes across diverse channel models, decoding algorithms, and scenarios of imperfect channel estimation. Furthermore, with the derived tight explicit bounds, optimizing constellation mapping design will be effective for improving Spinal codes. Additionally, the transmission pattern can be refined in the context of practical decoding algorithms. During validations of the proposed bound, we also noticed an error floor in Spinal codes' upper bounds at high SNR. Therefore, to reveal the reason behind the error floor and explicitly derive it may be an interesting work.

APPENDIX A

THE PROPERTIES OF HASH AND RELATED INFERENCES

The hash function is expressed as $\mathcal{H} : \{0, 1\}^v \times \{0, 1\}^k \rightarrow \{0, 1\}^v$. It introduces two properties as follows.

Property 1. As Perry et al. indicate [4], the hash function employed by Spinal codes should have pairwise independent

property:

$$\begin{aligned} & \Pr\{\mathcal{H}(\mathbf{s}, \mathbf{m}) = \mathbf{x}, \mathcal{H}(\mathbf{s}', \mathbf{m}') = \mathbf{x}'\} \\ &= \Pr\{\mathcal{H}(\mathbf{s}, \mathbf{m}) = \mathbf{x}\} \cdot \Pr\{\mathcal{H}(\mathbf{s}', \mathbf{m}') = \mathbf{x}'\} \\ &= 2^{-2v}, \end{aligned} \quad (82)$$

where $(\mathbf{s}, \mathbf{m}) \neq (\mathbf{s}', \mathbf{m}')$.

Property 2. A sufficiently large v leads to a zero-approaching hash collision probability, with

$$\begin{aligned} & \Pr\{\mathcal{H}(\mathbf{s}, \mathbf{m}) = \mathcal{H}(\mathbf{s}', \mathbf{m}')\} \\ &= \sum_{\mathbf{x} \in \{0,1\}^v} \underbrace{\Pr\{\mathcal{H}(\mathbf{s}, \mathbf{m}) = \mathbf{x}, \mathcal{H}(\mathbf{s}', \mathbf{m}') = \mathbf{x}'\}}_{\text{Property 1}} \\ &= 2^v \cdot 2^{-2v} = 2^{-v} \approx 0, \text{ iff } v \gg 0, \end{aligned} \quad (83)$$

where $(\mathbf{s}, \mathbf{m}) \neq (\mathbf{s}', \mathbf{m}')$ are arbitrary hash inputs.

The **Property 2** reveals that, given a sufficiently large v , distinct inputs to the hash function will almost surely yield distinct outputs.

Lemma 11. If $\mathbf{m}_i^* = \mathbf{m}'_i, \mathbf{s}_{i-1}^* = \mathbf{s}'_{i-1}$, then $\mathbf{s}_i^* = \mathbf{s}'_i, \forall i \in [n/k]$.

Proof. From (1), we could iteratively prove this lemma. \square

APPENDIX B

A. Proof of Corollary 1

The proof of is accomplished by re-deriving (9) as

$$\begin{aligned} & \int_{\mathbb{C}} \left[\sum_{x \in \Psi} \mathcal{Q}(x) \sqrt{f_Y(y | x, H)} \right]^2 dy \\ &= \frac{2^{-2c}}{\sqrt{2\pi\sigma^2}} \iint_{\mathbb{R}} \left[\sum_{x \in \Psi} \exp \left\{ -\frac{(Hy - x)^2}{4\sigma^2} \right\} \right]^2 dy \\ &= \sum_{\beta_i, \beta_j \in \Psi} \exp \left\{ -\frac{(H(\beta_i - \beta_j))^2}{8\sigma^2} \right\}. \end{aligned} \quad (84)$$

B. Proof of (11-(b))

The proof is equivalent to prove the following equality

$$\begin{aligned} & \int_{\mathbb{R}} \exp \left\{ -\frac{(a - a_1)^2 + (a - a_2)^2}{2\sigma^2} \right\} da \\ &= \exp \left\{ -\frac{(a_1 - a_2)^2}{4\sigma^2} \right\} \int_{\mathbb{R}} \exp \left\{ -\frac{(a - \frac{a_1 + a_2}{2})^2}{\sigma^2} \right\} da \\ &= \sqrt{\pi\sigma^2} \cdot \exp \left\{ -\frac{(a_1 - a_2)^2}{4\sigma^2} \right\}. \end{aligned} \quad (85)$$

APPENDIX C

A. Independence and Identically Distributed (i.i.d) $V_{i,j}$

To establish the i.i.d property of $V_{i,j} = h_{i,j}(f(\mathbf{x}_{i,j}(\mathbf{M}^*)) - f(\mathbf{x}_{i,j}(\mathbf{M}')))$, we consider each component separately. The i.i.d nature of $h_{i,j}$ is inherent in the flat fast fading scenario. For $f(\mathbf{x}_{i,j}(\mathbf{M}^*))$ and $f(\mathbf{x}_{i,j}(\mathbf{M}'))$, their i.i.d characteristics arise from the RNGs and hash functions used. The RNG, with

a consistent seed \mathbf{s}_i , ensures the independence of generated symbols, leading to the following lemma.

Lemma 12. For $\forall j \neq m$, and \mathbf{M} , the encoded symbol $f(\mathbf{x}_{i,j}(\mathbf{M}))$ is independent of $f(\mathbf{x}_{i,m}(\mathbf{M}))$.

The hash function \mathcal{H} ensures that the input and output of the function are independent with each other, i.e., $\forall 1 \leq i \leq n/k - 1$, \mathbf{s}_i is independent with \mathbf{s}_{i+1} . In this manner, due to the iteration structure with $\mathbf{s}_i = \mathcal{H}(\mathbf{s}_{i-1}, \mathbf{m}_i)$, we have

Lemma 13. For $\forall i \neq j$, it holds that \mathbf{s}_i is independent of \mathbf{s}_j .

With **Lemma 13** in hand, it is then very natural to establish the following corollary:

Lemma 14. For $\forall i \neq j$ and \mathbf{M} , the symbol $f(\mathbf{x}_{i,m}(\mathbf{M}))$ is independent of $f(\mathbf{x}_{j,m}(\mathbf{M}))$

Combing **Lemma 12** and **Lemma 14** together leads to the i.i.d characteristics of $f(\mathbf{x}_{i,j}(\mathbf{M}^*))$ and $f(\mathbf{x}_{i,j}(\mathbf{M}'))$.

B. Independence Between $h_{i,j}$, $f(\mathbf{x}_{i,j}(\mathbf{M}^*))$, and $f(\mathbf{x}_{i,j}(\mathbf{M}'))$

Since $h_{i,j}$ is the channel coefficient, it is natural to obtain that $h_{i,j}$ is independent with both $f(\mathbf{x}_{i,j}(\mathbf{M}^*))$, and $f(\mathbf{x}_{i,j}(\mathbf{M}'))$. The remaining issue is to establish that $f(\mathbf{x}_{i,j}(\mathbf{M}^*))$ is independent with $f(\mathbf{x}_{i,j}(\mathbf{M}'))$ for $i \geq a$ and $j \in [\ell_i]$, where $a \triangleq \min \{i | \mathbf{s}_i^* = \mathbf{s}'_i\}$. Before proving this, we first introduce the following lemma:

Lemma 15. If $\mathbf{m}_a^* \neq \mathbf{m}'_a$, then $\forall a \leq i \leq n/k$, $\Pr\{\mathbf{s}_i^* = \mathbf{s}'_i\} \leq 1 - (1 - 2^{-v})^{i-a+1}$.

Proof. Denote \mathcal{C}_i as the event that $\bigcap_{j=a}^i \mathbf{s}_j^* \neq \mathbf{s}'_j$, i.e., $\mathcal{C}_i \triangleq \left\{ \bigcap_{j=a}^i \mathbf{s}_j^* \neq \mathbf{s}'_j \right\}$. Then, by leveraging (83), we have

$$\Pr\{\mathcal{C}_a\} = 1 - 2^{-v}, \quad (86)$$

$$\Pr(\mathcal{C}_{i+1} | \mathcal{C}_i) = 1 - 2^{-v}, \text{ for } \forall a \leq i \leq n/k - 1,$$

Therefore, since $\mathcal{C}_i \subset \mathcal{C}_{i-1}$, we have the recursive relation:

$$\begin{aligned} \Pr(\mathcal{C}_i) &= \Pr(\mathcal{C}_i | \mathcal{C}_{i-1}) \Pr(\mathcal{C}_{i-1}) \\ &= (1 - 2^{-v}) \Pr(\mathcal{C}_{i-1}). \end{aligned} \quad (87)$$

By iteratively leveraging the above recursive relation and $\Pr\{\mathcal{C}_a\} = 1 - 2^{-v}$, we have

$$\Pr(\mathcal{C}_i) = (1 - 2^{-v})^{i-a+1}. \quad (88)$$

From (83) we know that

$$\Pr(\mathbf{s}_i^* = \mathbf{s}'_i | \mathcal{C}_{i-1}) = \Pr(\mathbf{s}_i^* = \mathbf{s}'_i | \mathbf{s}_{i-1} \neq \mathbf{s}'_{i-1}) = 2^{-v}. \quad (89)$$

We then establish the recursive inequality relationship between $\Pr\{\mathbf{s}_i^* = \mathbf{s}'_i\}$ and $\Pr\{\mathbf{s}_{i-1}^* = \mathbf{s}'_{i-1}\}$ by leveraging the inequality $\Pr\{A \cap B\} \leq \Pr\{A\}$ and applying (88) and (89):

$$\begin{aligned} \Pr\{\mathbf{s}_i^* = \mathbf{s}'_i\} &= \Pr(\mathcal{C}_{i-1}, \mathbf{s}_i^* = \mathbf{s}'_i) + \Pr(\overline{\mathcal{C}_{i-1}}, \mathbf{s}_i^* = \mathbf{s}'_i) \\ &\leq \Pr(\mathcal{C}_{i-1}) \Pr(\mathbf{s}_i^* = \mathbf{s}'_i | \mathcal{C}_{i-1}) + \Pr(\mathbf{s}_{i-1} = \mathbf{s}'_{i-1}, \mathbf{s}_i^* = \mathbf{s}'_i) \\ &\leq (1 - 2^{-v})^{i-a} \cdot 2^{-v} + \Pr(\mathbf{s}_{i-1}^* = \mathbf{s}'_{i-1}). \end{aligned} \quad (90)$$

Iterating (90) yields the inequality relationship in **Lemma 15**:

$$\Pr\{\mathbf{s}_i^* = \mathbf{s}'_i\} \leq \sum_{j=a}^i (1 - 2^{-v})^{j-a} \cdot 2^{-v} = 1 - (1 - 2^{-v})^{i-a+1}. \quad (91)$$

With **Lemma 15**, we adopt the sandwich theorem and have

$$0 \leq \lim_{v \rightarrow \infty} \Pr \{ \mathbf{s}_i^* = \mathbf{s}'_i \} \leq \lim_{v \rightarrow \infty} 1 - (1 - 2^{-v})^{i-a+1} = 0. \quad (92)$$

Consequently, it follows that $\lim_{v \rightarrow \infty} \Pr (\mathbf{s}_i^* = \mathbf{s}'_i) = 0$. Therefore, for all $a \leq i \leq n/k$, we can assert that $\mathbf{s}_i^* \neq \mathbf{s}'_i$ in scenarios with sufficiently large v . This leads to that for $\forall a \leq i \leq n/k$, $f(\mathbf{x}_{i,j}(\mathbf{M}'))$ is independent of $f(\mathbf{x}_{i,j}(\mathbf{M}^*))$.

APPENDIX D PROOF OF (73)

Note that $\theta_t \leq \pi/2$, we have

$$\begin{aligned} & \sum_{t \in [N]} b_t \left(\sum_{\beta_i, \beta_j \in \Psi} 2^{-2c} \mathbb{E}_H \left[\exp \left\{ \frac{-|H(\beta_i - \beta_j)|^2}{4\sigma^2 \sin^2 \theta_t} \right\} \right] \right)^{L_a} \\ & \leq \sum_{t \in [N]} b_t \left(\sum_{\beta_i, \beta_j \in \Psi} 2^{-2c} \mathbb{E}_H \left[\exp \left\{ \frac{-|H(\beta_i - \beta_j)|^2}{4\sigma^2} \right\} \right] \right)^{L_a} \\ & = \left(\sum_{\beta_i, \beta_j \in \Psi} 2^{-2c} \mathbb{E}_H \left[\exp \left\{ \frac{-|H(\beta_i - \beta_j)|^2}{4\sigma^2} \right\} \right] \right)^{L_a} \sum_{t \in [N]} b_t. \end{aligned} \quad (93)$$

Note that $\sum_{t \in [N]} b_t = 1/2$, we thus establish the inequality.

REFERENCES

- [1] X. Chen, A. Li, and S. Wu, "Tight upper bounds on the error probability of spinal codes over fading channels," in *Proc. IEEE ISIT*, 2023, pp. 1277–1282.
- [2] J. Perry, H. Balakrishnan, and D. Shah, "Rateless Spinal Codes," *Proc. ACM HotNets*, pp. 1–6, 2011.
- [3] H. Balakrishnan, P. Iannucci, J. Perry, and D. Shah, "De-randomizing Shannon: The design and analysis of a capacity-achieving rateless code," *arXiv preprint arXiv:1206.0418*, 2012.
- [4] J. Perry, P. A. Iannucci, K. E. Fleming, H. Balakrishnan, and D. Shah, "Spinal Codes," *Proc. ACM SIGCOMM 2012*, pp. 49–60, 2012.
- [5] A. Shokrollahi, "Raptor codes," *IEEE Trans. Inf. Theory*, vol. 52, no. 6, pp. 2551–2567, 2006.
- [6] R. Palanki and J. Yedidia, "Rateless codes on noisy channels," *Proc. IEEE ISIT*, p. 37, 2004.
- [7] A. Gudipati and S. Katti, "Strider: Automatic Rate Adaptation and Collision Handling," *Proc. ACM SIGCOMM 2011*, pp. 158–169, 2011.
- [8] R. Gallager, "Low-density parity-check codes," *IRE Trans. Inf. Theory*, vol. 8, no. 1, pp. 21–28, 1962.
- [9] X. Yu, Y. Li, W. Yang, and Y. Sun, "Design and Analysis of Unequal Error Protection Rateless Spinal Codes," *IEEE Trans. Commun.*, vol. 64, no. 11, pp. 4461–4473, 2016.
- [10] X. Yu, Y. Li, and W. Yang, "Superposition spinal codes with unequal error protection property," *IEEE Access*, vol. 5, pp. 6589–6599, 2017.
- [11] W. Yang, Y. Li, X. Yu, and Y. Sun, "Two-way spinal codes," in *Proc. IEEE ISIT*, 2016, pp. 1919–1923.
- [12] Y. Hu, R. Liu, H. Bian, and D. Lyu, "Design and analysis of a low-complexity decoding algorithm for spinal codes," *IEEE Trans. Veh. Technol.*, vol. 68, no. 5, pp. 4667–4679, 2019.
- [13] W. Yang, Y. Li, X. Yu, and J. Li, "A low complexity sequential decoding algorithm for rateless spinal codes," *IEEE Commun. Lett.*, vol. 19, no. 7, pp. 1105–1108, 2015.
- [14] Y. Li, J. Wu, B. Tan, M. Wang, and W. Zhang, "Compressive spinal codes," *IEEE Trans. Veh. Technol.*, vol. 68, no. 12, pp. 11944–11954, 2019.
- [15] J. Xu, S. Wu, J. Jiao, and Q. Zhang, "Optimized puncturing for the spinal codes," in *Proc. IEEE ICC*, 2019, pp. 1–5.
- [16] A. Li, S. Wu, Y. Wang, J. Jiao, and Q. Zhang, "Spinal codes over BSC: Error probability analysis and the puncturing design," in *Proc. IEEE VTC2020-Spring*, 2020, pp. 1–5.
- [17] S. Meng, S. Wu, A. Li, J. Jiao, N. Zhang, and Q. Zhang, "Analysis and Optimization of Spinal Codes over the BSC: from the AoI Perspective," in *IEEE ICC Workshops*. IEEE, 2021, pp. 1–6.
- [18] —, "Analysis and optimization of the harq-based spinal coded timely status update system," *IEEE Trans. Commun.*, vol. 70, no. 10, pp. 6425–6440, 2022.
- [19] X. Xu, S. Wu, D. Dong, J. Jiao, and Q. Zhang, "High performance short polar codes: A concatenation scheme using spinal codes as the outer code," *IEEE Access*, vol. 6, pp. 70644–70654, 2018.
- [20] H. Liang, A. Liu, X. Tong, and C. Gong, "Raptor-like rateless spinal codes using outer systematic polar codes for reliable deep space communications," in *IEEE INFOCOM Workshops*, 2020, pp. 1045–1050.
- [21] D. Dong, S. Wu, X. Jiang, J. Jiao, and Q. Zhang, "Towards high performance short polar codes: concatenated with the spinal codes," in *Proc. IEEE PIMRC*, 2017, pp. 1–5.
- [22] Y. Cao, F. Du, J. Zhang, and X. Peng, "Polar-uep spinal concatenated encoding in free-space optical communication," *Applied Optics*, vol. 61, no. 1, pp. 273–278, 2022.
- [23] S. Yousefi and A. Khandani, "A new upper bound on the ML decoding error probability of linear binary block codes in AWGN interference," *IEEE Trans. Inf. Theory*, vol. 50, no. 12, pp. 3026–3036, 2004.
- [24] D. Goldin and D. Burshtein, "Performance Bounds of Concatenated Polar Coding Schemes," *IEEE Trans. Inf. Theory*, vol. 65, no. 11, pp. 7131–7148, 2019.
- [25] B. Shuval and I. Tal, "A Lower Bound on the Probability of Error of Polar Codes over BMS Channels," *IEEE Trans. Inf. Theory*, vol. 65, no. 4, pp. 2021–2045, 2019.
- [26] T. Duman and M. Salehi, "New performance bounds for turbo codes," *IEEE Trans. Commun.*, vol. 46, no. 6, pp. 717–723, 1998.
- [27] F. Lázaro, G. Liva, G. Bauch, and E. Paolini, "Bounds on the Error Probability of Raptor Codes Under Maximum Likelihood Decoding," *IEEE Trans. Inf. Theory*, vol. 67, no. 3, pp. 1537–1558, 2021.
- [28] B. Schotsch, G. Garramone, and P. Vary, "Analysis of LT Codes over Finite Fields under Optimal Erasure Decoding," *IEEE Commun. Lett.*, vol. 17, no. 9, pp. 1826–1829, 2013.
- [29] B. Schotsch, *Rateless coding in the finite length regime*. Hochschulbibliothek der Rheinisch-Westfälischen Technischen Hochschule Aachen, 2014.
- [30] I. Sason and S. Shamai, "Performance Analysis of Linear Codes under Maximum-Likelihood Decoding: A Tutorial," *Foundations and Trends in Communications and Information Theory*, vol. 3, no. 1–2, pp. 1–222, 2006.
- [31] Y. Polyanskiy, H. V. Poor, and S. Verdú, "Channel coding rate in the finite blocklength regime," *IEEE Trans. Inf. Theory*, vol. 56, no. 5, pp. 2307–2359, 2010.
- [32] R. G. Gallager, *Information theory and reliable communication*. Wiley, 1968, vol. 588.
- [33] A. Li, S. Wu, J. Jiao, N. Zhang, and Q. Zhang, "New Upper Bounds on the Error Probability under ML Decoding for Spinal Codes and the Joint Transmission-Decoding System Design," *arXiv preprint arXiv:2101.07953*, 2021.
- [34] A. Li, S. Wu, J. Jiao, N. Zhang, and Q. Zhang, "Spinal Codes Over Fading Channel: Error Probability Analysis and Encoding Structure Improvement," *IEEE Trans. Wirel. Commun.*, vol. 20, no. 12, pp. 8288–8300, 2021.
- [35] A. Karadimitrakis, A. L. Moustakas, and R. Couillet, "Gallager Bound for MIMO Channels: Large- N Asymptotics," *IEEE Trans. Wirel. Commun.*, vol. 17, no. 2, pp. 1323–1330, 2017.
- [36] D. Tse and P. Viswanath, *Fundamentals of wireless communication*. England: Cambridge University Press, 2005.
- [37] J. W. Craig, "A new, simple and exact result for calculating the probability of error for two-dimensional signal constellations," in *Proc. IEEE MILCOM*, 1991, pp. 571–575.